Title : Induction of photosynthetic carbon fixation in anoxia relies on hydrogenase activity and PGRL1-mediated cyclic electron flow in *Chlamydomonas reinhardtii.*

Short Title: Photosynthesis induction in anoxic Chlamydomonas

Damien Godaux[1], Benjamin Bailleul[1], Nicolas Berne[1], Pierre Cardol[1§]

Author affiliation: [1] Genetics and Physiology of microalgae, PhytoSYSTEMS, Department of Life Sciences, University of Liège, B-4000 Liège, Belgium.

[§]To whom correspondence should be addressed:

Pierre Cardol. Bvd du Rectorat, 27, B22, Institute of Botany, Dept of Life Sciences, University of Liège, 4000 Liège, Belgium. pierre.cardol@ulg.ac.be. Tel +32 (0)43663840. ORCIDs, 0000-0001-9799-0546

Estimate of the length : 9 pages

ABSTRACT

The model green microalga *Chlamydomonas reinhardtii* is frequently subject to periods of dark and anoxia in its natural environment. Here, by resorting to mutants defective in the maturation of the chloroplastic oxygen-sensitive hydrogenases or in PGRL1-dependent cyclic electron flow around photosystem I (PSI-CEF), we demonstrate the sequential contribution of these alternative electron flows (AEF) in the reactivation of photosynthetic carbon fixation during a shift from dark-anoxia to light. At light onset, hydrogenase activity sustains a linear electron flow (LEF) from photosystem II (PSII) which is followed by a transient PSI-CEF in wild type. By promoting ATP synthesis without net generation of photosynthetic reductants, the two AEF are critical for restoration of the capacity for carbon dioxide fixation in the light. Our data also suggest that the decrease in hydrogen evolution with time of illumination might be due to competition for reduced ferredoxins between ferredoxin-NADPH oxidoreductase (FNR) and hydrogenases, rather than due to the sensitivity of hydrogenase activity to oxygen. Finally, the absence of the two alternative pathways in a double mutant *pgrl1 hydg-2* is detrimental for photosynthesis and growth, and cannot be compensated by any other AEF or anoxic metabolic responses. This highlights the role of hydrogenase activity and PSI-CEF in the ecological success of microalgae in low-oxygen environments.

One sentence summary

Photosynthesis and growth in anoxia critically depends at least on hydrogenase-dependent linear electron flow or PGRL-dependent PSI-cyclic electron flow in the green alga *Chlamydomonas reinhardtii*.

Keywords: Hydrogenase, Cyclic electron flow, Chlamydomonas, Anoxia

INTRODUCTION

Unicellular photosynthetic organisms like the green alga *Chlamydomonas reinhardtii* frequently experience anoxic conditions in their natural habitat, especially during the night when the microbial community consumes the available oxygen. Under anoxia, lack of ATP synthesis by F_1F_O ATP synthase due to the absence of mitochondrial respiration is compensated by the activity of various plant-type and bacterial-type fermentative enzymes that drive a sustained glycolytic activity (Mus et al., 2007; Terashima et al., 2010; Grossman et al., 2011; Yang et al., 2014). In *C. reinhardtii*, upstream glycolytic enzymes including the reversible glyceraldehyde 3-phosphate dehydrogenase are located in the chloroplast (Johnson and Alric, 2012). This last enzyme is shared by the glycolysis (oxidative activity) and the Calvin-Benson-Bassham (CBB) cycle (reductive activity) (Johnson and Alric, 2013). In dark anoxic conditions, the CBB cycle is inactive thus avoiding wasteful using up of available ATP and depletion of the required intermediates for glycolysis. On the other side, ability of microalgae to perform photosynthetic carbon fixation when transferred from dark to light in the absence of oxygen might also be critical for adaptation to their environment. In such conditions, not only the LEF to RubisCO but also AEF towards oxygen (chlororespiration, Mehler reaction, mitochondrial respiration) (reviewed in (Cardol et al., 2011; Miyake, 2010; Peltier et al., 2010)) are impaired. Thus, cells need to circumvent a paradoxical situation: the activity of the CBB cycle requires the restoration of the cellular ATP but the chloroplastic CF_1F_O ATP synthase activity is compromised by the impairment of most of the photosynthetic electron flows that usually generate the proton motive force in oxic conditions. Other AEF, specific to anoxic conditions, should therefore be involved to promote ATP synthesis without net synthesis of NADPH and explain the light-induced restoration of CBB cycle activity.

Among enzymes expressed in anoxia, the oxygen-sensitive hydrogenases (HYDA1 and HYDA2 in *Chlamydomonas*) catalyse the reversible reduction of protons into molecular hydrogen from the oxidation of reduced ferredoxins (FDX) (Florin et al., 2001). Although hydrogen metabolism in microalgae has been largely studied in the last 15 years in perspective of promising future renewable energy carriers (e.g. (Melis et al., 2000; Kruse et al., 2005; Ghirardi et al., 2009)), the physiological role of such an oxygen-sensitive enzyme linked to the photosynthetic pathway has been poorly considered. The forty-years ago proposal that H_2 evolution by hydrogenase is involved in induction of photosynthetic electron transfer after anoxic incubation (Kessler, 1973; Schreiber and Vidaver, 1974) has been only recently demonstrated in *C. reinhardtii*. Gas exchange measurements indeed showed that H_2 evolution occurs prior CO_2 fixation upon illumination (Cournac et al., 2002). At light onset after a prolonged period in dark anoxic conditions, the photosynthetic electron flow is mainly a LEF towards hydrogenase (Godaux et al., 2013) and lack of hydrogenase activity in *hydEF* mutant strain

deficient in hydrogenases maturation (Posewitz et al., 2004) induces a lag in induction of PSII activity (Ghysels et al., 2013). In cyanobacteria, the bidirectional Ni-Fe hydrogenase might also work as an electron valve for disposal of electrons generated at the onset of illumination of cells (Cournac et al., 2004) or when excess electrons are generated during photosynthesis, preventing the slowing of the electron transport chain under stress conditions (Carrieri et al., 2011; Appel et al., 2000). The bidirectional Ni-Fe hydrogenase could also dispose of excess of reducing equivalents during fermentation in dark anaerobic conditions, helping to generate ATP and maintaining homeostasis (Barz et al., 2010). A similar role for hydrogenase in setting the redox poise in the chloroplast of *Chlamydomonas reinhardtii* in anoxia has been recently uncovered (Clowez et al., 2015).

Still, the physiological and evolutionary advantages of hydrogenase activity have not been demonstrated so far and the mechanism responsible for the cessation of hydrogen evolution remains unclear. In this respect, at least three hypotheses have been formulated : (i) the inhibition of hydrogenase by O_2 produced by water photolysis (Ghirardi et al., 1997; Cohen et al., 2005), (ii) the competition between FNR and hydrogenase activity for reduced FDX (Yacoby et al., 2011), and (iii) the inhibition of electron supply to hydrogenases by the proton gradient generated by another AEF, the cyclic electron flow around PSI (Tolleter et al., 2011). Firstly described by Arnon in the middle 1950's (Arnon, 1955), PSI-CEF consists in a reinjection of electrons from reduced FDX or NADPH pool in the plastoquinone (PQ) pool. By generating an additional trans-thylakoidal proton gradient without producing reducing power, this AEF thus contributes to adjust the ATP/NADPH ratio for carbon fixation in various energetic unfavourable conditions including anoxia (Tolleter et al., 2011; Alric, 2014), high light (Tolleter et al., 2011; Johnson et al., 2014), or low CO_2 (Lucker and Kramer, 2013). In *C. reinhardtii* two pathways have been suggested to be involved in PSI-CEF: (i) a type II NAD(P)H dehydrogenase (NDA2) (Jans et al., 2008) driving the electrons from NAD(P)H to the PQ pool, and (ii) a pathway involving Proton Gradient Regulation (PGR) proteins where electrons from reduced ferredoxins return to PQ pool or cytochrome b_6f. Not fully understood, this latter pathway comprises at least PGR5 and PGRL1 proteins (Tolleter et al., 2011; Johnson et al., 2014; Iwai et al., 2010) and is the major route for PSI-CEF in *C. reinhardtii* cells placed in anoxia (Alric, 2014).

In the present work, we took advantage of specific *C. reinhardtii* mutants defective in hydrogenase activity and PSI-CEF to study photosynthetic electron transfer after a period of dark-anoxic conditions. Based on biophysical and physiological complementary studies, we demonstrate that at least hydrogenase activity or PSI-CEF is compulsory for the activity of CBB cycle and for the survival of the cells submitted to anoxic conditions in their natural habitat.

RESULTS AND DISCUSSION

In anoxia, induction of PSII electron flow requires at least hydrogenase activity or PSI-cyclic electron flow.

To explore the interplay between hydrogenase activity, PSI-CEF and CBB cycle activity in *Chlamydomonas reinhardtii* in anoxia, we resorted to *pgrl1 mt-* nuclear mutant defective in PSI-CEF (Tolleter et al., 2011) and to *hydg-2 mt+* nuclear mutant deprived of hydrogenase activity due to the lack of HYDG maturation factor (Godaux et al., 2013). We also isolated double mutants impaired in both AEF by crossing the *pgrl1* and *hydg*-2 single mutants (Supplemental Figure 1). Results will be shown for one meiotic product (B1-21), named by convenience *pgrl1 hydg-2* in this report, but every double mutant meiotic product had the same behavior (Supplemental Figure 1). Similarly, both wild-type strains from which derived the single mutants have been compared for each parameter assessed in the present work and did not show any difference (Tables 1 and 2). Data presented refer to the parental wild-type strain of *hydg-2* mutant.

Induction of photosynthetic electron transfer in the wild type and the three mutant strains (*pgrl1, hydg-2, pgrl1 hydg*-2) was investigated. As an exciting light intensity, we choose a near saturating light intensity (250 µmol photons $\cdot$ m^{-2} $\cdot$ s^{-1}) corresponding to ~100 e^- $\cdot$ s^{-1} $\cdot$ $PSII^{-1}$ in oxic conditions (Table 1). In this range of light intensities, growth and photosynthesis of aerated cultures were similar for all the strains (Table 1). After one hour of acclimation to dark and anoxia, a time required for proper expression and activity of hydrogenases (Forestier et al., 2003; Godaux et al., 2013) (Supplemental Figure 2), we measured the hydrogen production rate (J_{H2}), the yield of PSII and PSI (ϕ_{PSII}, ϕ_{PSI}), as well as the mean photochemical rate based on electrochromic shift (ECS) measurements (R_{ph}) at the onset of light (10 seconds) (Table 2). In the two wild-type strains, in the *pgrl1* mutant and in the *PGRL1* complemented strain, R_{ph} was about 20 e^- $\cdot$ s^{-1} $\cdot$ PS^{-1} and J_{H2} was about 20 e^- $\cdot$ s^{-1} $\cdot$ PSI^{-1}, which represents about 40 % of the maximal capacity measured for hydrogenase (Godaux et al., 2013). In wild-type, 20 e^- $\cdot$ s^{-1} $\cdot$ PSI^{-1} corresponds to an H_2 production rate of 0.58 µmoles H_2 $\cdot$ mg chlorophyll^{-1} $\cdot$ min^{-1}, which is compatible with recent published values of ~0.25-0.36 µmoles H_2 $\cdot$ mg chlorophyll^{-1} $\cdot$ min^{-1} (Tolleter et al., 2011; Clowez et al., 2015). On the contrary, in the two mutants lacking hydrogenase activity (*hydg-2* and *pgrl1 hydg-2)*, neither hydrogen production, nor significant photosynthetic activity was detected after 10 seconds of illumination (Table 2). The lack of PSII-driven electron flow in hydrogenase mutants (*hydg-2* and *pgrl1 hydg-2*) and the similar activities in wild type and *pgrl1* indicate that in this time range the activities of PSI and PSII are mainly dependent on the presence of the hydrogenases, in agreement with our previous results (Godaux et

Table 1. **Growth rate, photosynthetic features and starch content in oxic conditions**.

	Growth rate	Φ_{PSII}	ETR_{PSII}	PSI/PSII	Starch content
wt (*1'*)	0.54 ± 0.04	0.50 ± 0.02	100 ± 4	1.35 ± 0.23	0.68 ± 0.19
wt (*137C*)	0.56 ± 0.03	0.51 ± 0.02	102 ± 4	1.21 ± 0.18	1.95 ± 0.68
pgrl1	0.58 ± 0.08	0.49 ± 0.03	98 ± 6	1.16 ± 0.29	1.87 ± 0.65
hyg-2	0.50 ± 0.07	0.50 ± 0.01	100 ± 3	1.33 ± 0.21	0.59 ± 0.10
pgrl1 hydg-2	0.54 ± 0.05	0.51 ± 0.02	102 ± 4	1.11 ± 0.15	1.99 ± 0.22

Growth rate (μ, day^{-1}) in mixotrophic conditions (TAP, acetate, continuous light). Φ_{PSII}, PSII quantum yield. ETR_{PSII}, PSII electron transfer rate ($e^- \cdot s^{-1} \cdot PSII^{-1}$). A Φ_{PSII} of 0.5 corresponds to an ETR_{PSII} of ~ 100 $e^- \cdot s^{-1} \cdot PSII^{-1}$. PSI/PSII stoichiometry, the ratio between active PSI and PSII centers was estimated as described in Cardol et al., 2009 (see methods for further information). Starch content ($pg \cdot cell^{-1}$). All measurements were performed at 250 μmol photons $\cdot m^{-2} \cdot s^{-1}$ at least in triplicate ($n \geq 3$) and data are presented as means ± SD. Wild type *1'* derives from *137c* reference wild-type strain and is the parental strain of *hydg-2* (Godaux et al., 2013). Wild type *137c* is the parental strain of *pgrl1* (Tolleter et al., 2011).

al., 2013). By acting as an electron safety valve, hydrogenases thus allow a LEF from PSII and PSI and sustain the generation of an electrochemical proton gradient for subsequent ATP synthesis.

Table 2. **Photosynthetic parameters upon a shift from dark-anoxia (1 hour) to light (10 seconds)**.

	J_{H2}	R_{ph}	Φ_{PSII}	Φ_{PSI}
wt (*1'*)	19.8 ± 4.4	18.9 ± 8.1	0.12 ± 0.04	0.21 ± 0.04
wt (*137C*)	18.1 ± 6.2	19.2 ± 5.6	0.11 ± 0.01	0.18 ± 0.06
pgrl1	17.0 ± 7.1	17.4 ± 3.6	0.09 ± 0.02	0.19 ± 0.07
hyg-2	1.7 ± 2.1	3.8 ± 2.4	0.03 ± 0.02	0.04 ± 0.02
pgrl1 hydg-2	0.9 ± 2.5	4.1 ± 1.2	0.01 ± 0.01	0.02 ± 0.03
pgrl1**::PGRL1**	21.3 ± 6.5	n.d.	0.13 ± 0.04	n.d.

J_{H2}, hydrogen evolution rate ($e^- \cdot s^{-1} \cdot PSI^{-1}$). R_{ph}, photochemical rate ($e^- \cdot s^{-1} \cdot PS^{-1}$). Φ_{PSII}, PSII quantum yield. Φ_{PSI}, PSI quantum yield. All measurements were performed at 250 µmol photons $\cdot m^{-2} \cdot s^{-1}$ at least in triplicate (n ≥ 3) and data are presented as means ± SD. Wild type *1'* derives from *137c* reference wild-type strain and is the parental strain of *hydg-2* (Godaux et al., 2013). Wild type *137c* is the parental strain of *pgrl1* (Tolleter et al., 2011). The *pgrl1*::PGRL1 strain is the complemented strain of *pgrl1* (Tolleter et al., 2011). n.d., not determined.

Accordingly, we assumed that the values of ϕ_{PSII}^{1} and ϕ_{PSI} after 10 seconds of illumination correspond to 20 $e^- \cdot s^{-1} \cdot PS^{-1}$ and used these values as a ruler to calculate the electron transfer rates through PSI (ETR_{PSI} in $e^- \cdot s^{-1} \cdot PSI^{-1}$) and PSII ($ETR_{PSII}$ in $e^- \cdot s^{-1} \cdot PSII^{-1}$) for longer times (see methods for further details).

When the wild type was illuminated for a longer time, the hydrogen production dropped to zero after about 200 seconds, followed by an increase of ETR_{PSII} (Figure 1A). In *hydg-2* strain, J_{H2} and ETR_{PSII} were below detection during the first two minutes of illumination (Figure 1C), as previously reported (Godaux et al., 2013; Ghysels et al., 2013), but ETR_{PSII} increased later. In the *pgrl1* mutant, J_{H2} decreased very slowly, in agreement with previous observations (Tolleter et al., 2011), together with a slow increase of ETR_{PSII} (Figure 1B). Thus, after 10 minutes of illumination, photosynthetic activity partially recovered in wild type and single mutants. In contrast, ETR_{PSII} in *pgrl1 hydg-2* double mutants remained null for the duration of the experiment (Figure 1D and Supplemental Figure 3).

Such an increase of ETR_{PSII} is usually ascribed to the activation of the CBB cycle (Cournac et al., 2002). However some electrons originated from PSII might also be rerouted towards O_2 reduction (PSI-Mehler reaction, mitochondrial respiration, etc). To test these possibilities, we added prior to illumination, glycolaldehyde, an effective inhibitor of phosphoribulokinase (Sicher, 1984) or carbonyl cyanide *m*-chlorophenyl hydrazone (CCCP), an uncoupler of membrane potential preventing ATP synthesis in mitochondria and chloroplasts. In the presence of these inhibitors, both J_{H2} and ETR_{PSII} remained stable in wild type as well as in single mutants for the duration of the experiment (Figure 2). These results confirm that (i) the hydrogenase is the main electron sink for PSII-originated electrons when CBB cycle is inactive, (ii) the increase of ETR_{PSII} corresponds to the redirection of the LEF to CBB cycle activity at the expense of hydrogenase activity and (iii) this increase depends on the presence of an electrochemical proton gradient for ATP synthesis.

As a consequence, we can reasonably assume that the divergence between J_{H2} and ETR_{PSII} is mainly indicative of an electron flux towards CBB cycle (*i.e.* CO_2 fixation through $NADP^+$ reduction, J_{CO2} in $e^- \cdot s^{-1} \cdot PSI^{-1}$). More formally, ETR_{PSII} is the sum of only two components: (i) ETR_{PSII} towards H_2 evolution (J_{H2}) and (ii) ETR_{PSII} towards CO_2 fixation (J_{CO2}). Thus $J_{CO2} = ETR_{PSII} - J_{H2}$ (Figures 1 and 2). Such an indirect calculation of J_{CO2} is correct only if PSI/PSII ratio is 1, which is not the case for all strains (Table 1). In an attempt to simplify calculations, we assumed in the following that PSI/PSII stoichiometry is 1. This indicates that in wild type and single mutants, electrons from PSII are progressively routed towards CO_2 fixation (Figure 1).

We also performed calculations taking into account PSI/PSII stoichiometry measured in Table 1. For wild type 1', that has the largest PSI/PSII ratio (~1.3), photosynthetic electron flows are modified at most by 15 % (see methods for further information).

Transitory induction of PGRL1-dependent PSI-CEF upon illumination in anoxia.

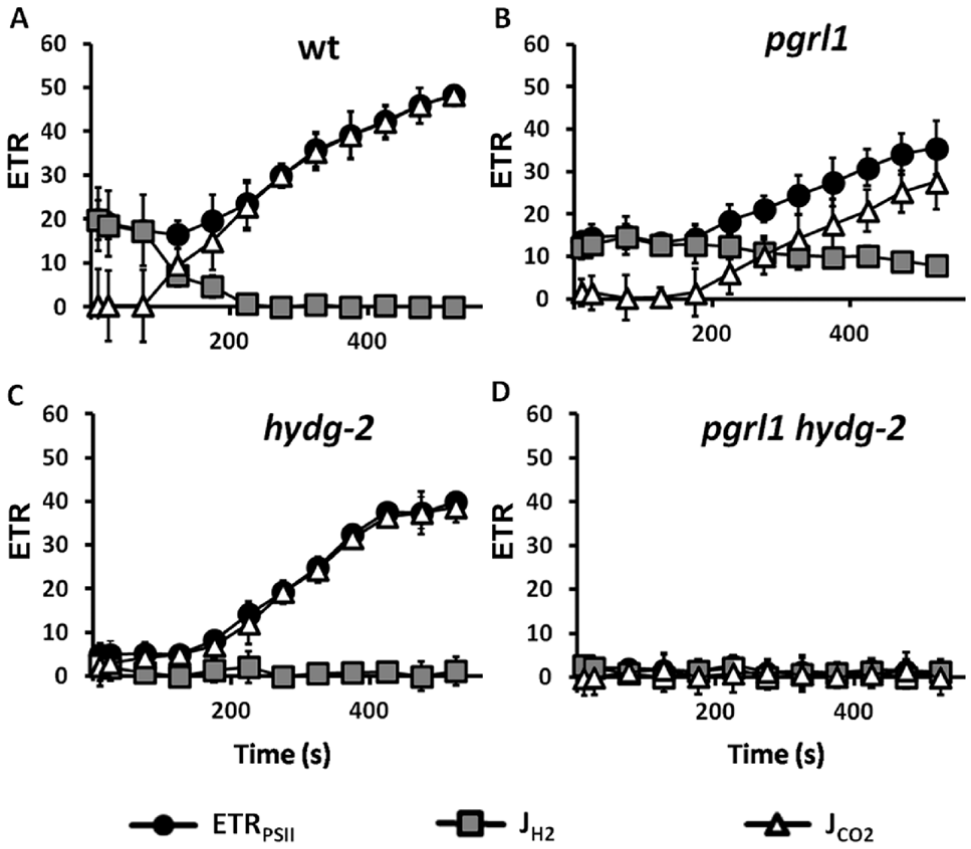

Figure 1. Activities of PSII, hydrogenases and CBB upon a shift from dark-anoxia (1 hour) to light (250 µmol photons · m^{-2} · s^{-1}) in wild type (*A*), *pgrl1* (*B*), *hydg-2* (*C*), and *pgrl1 hydg-2* (*D*). **ETR**, electron transport rate. Dark circles, PSII electron transfer rate (ETR_{PSII}, e^- · s^{-1} · $PSII^{-1}$); grey squares, hydrogen evolution rate (J_{H2}, e^- · s^{-1} · PSI^{-1}); open triangle, electron flow towards carbon fixation (J_{CO2}, e^- · s^{-1} · PSI^{-1}) calculated as follow: $J_{CO2} = ETR_{PSII} - J_{H2}$ (see text for further information). All measurements were performed at least in triplicate (n ≥ 3) and data are presented as means ± SD.

1

As indicated by the previous results, the presence of PGRL1 is necessary for the reactivation of the CBB cycle, in the absence of hydrogenase activity. It is generally acknowledged that the PGRL1 protein participates to PSI-CEF both in *Chlamydomonas* and *Arabidopsis* (DalCorso et al., 2008; Tolleter et al., 2011; Hertle et al., 2013; Johnson et al., 2014; Iwai et al., 2010). By generating an

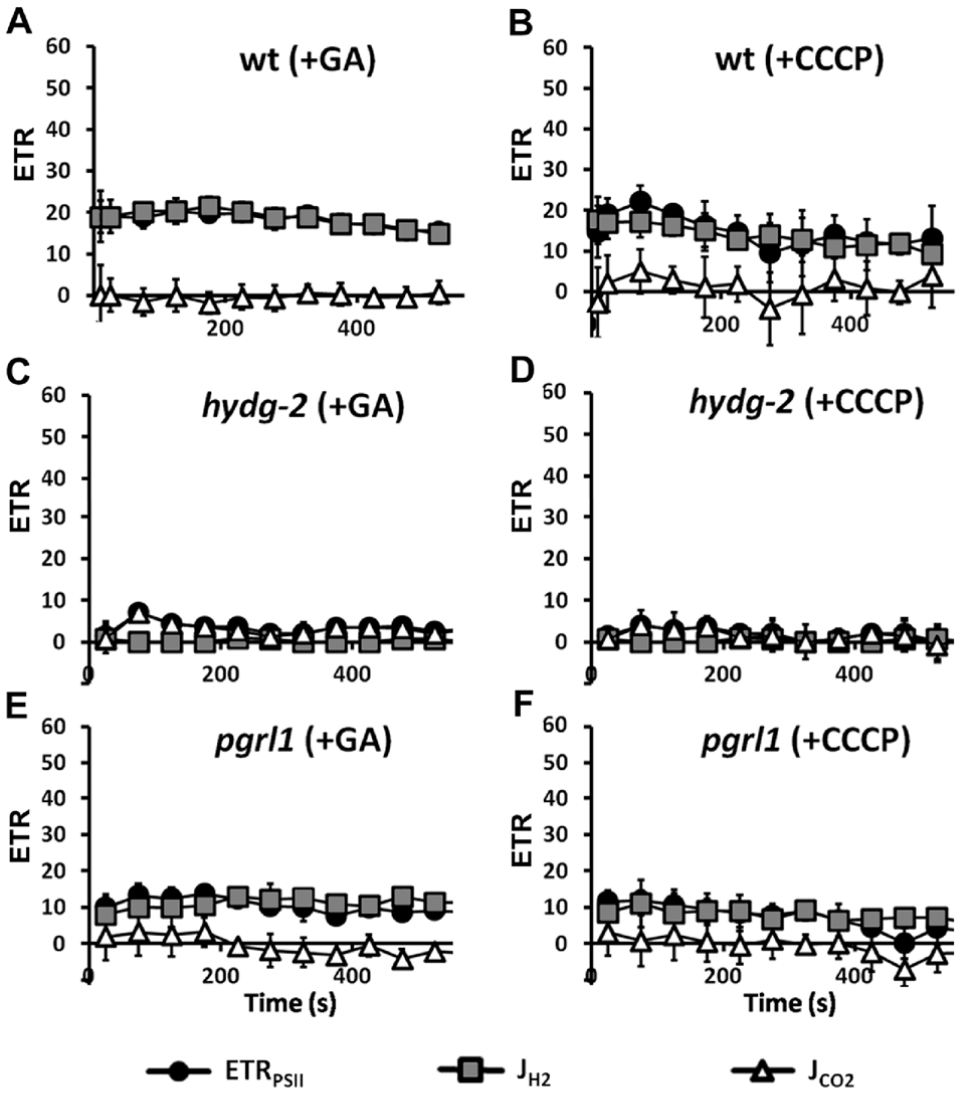

Figure 2. Activities of PSII, hydrogenases and CBB upon a shift from dark-anoxia (1 hour) to light (250 µmol photons · m^{-2} · s^{-1}) in wild type (A, B), *hydg-2* (C, D) and *pgrl1* (E, F) in conditions of inhibition of the CBB cycle. Glycolaldehyde (GA, 10mM) (*A*, *C*, *E*), or carbonyl cyanide m-chlorophenyl hydrazone (CCCP, 20µM) (*B*, *D*, *F*) were added prior illumination. **ETR**, electron transport rate. Dark circles, PSII electron transfer rate (ETR_{PSII}, e^- · s^{-1} · $PSII^{-1}$); gray squares, hydrogen evolution rate (J_{H2}, e^- · s^{-1} · PSI^{-1}); open triangle, electron flow towards carbon fixation (J_{CO2}, e^- · s^{-1} · PSI^{-1}) calculated as follow: $J_{CO2} = ETR_{PSII} - J_{H2}$ (see text for further information). All measurements were performed at least in triplicate (n ≥ 3) and data are presented as means ± SD.

[1]additional proton motive force, PSI-CEF is proposed to enhance ATP synthesis in the illuminated chloroplast (Allen, 2003) and/or to trigger photoprotection of the photosynthetic apparatus (Joliot and Johnson, 2011; Tikkanen et al., 2012). Occurrence of PSI-CEF has been a matter of debate during the last decade, mainly because most experiments have been performed in non-physiological

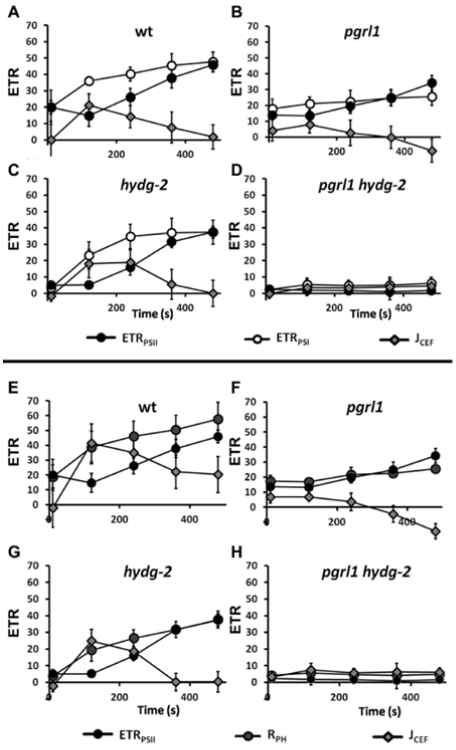

Figure 3. PSI cyclic electron flow upon a shift from dark-anoxia (1 hour) to light in wild type (A, E), *pgrl1* (B, F), *hydg-2* (C, G) and *pgrl1 hydg-2* (D, H). **ETR**, electron transport rate. Dark circles, PSII electron transfer rate (A-H) (ETR_{PSII}, $e^- \cdot s^{-1} \cdot PSII^{-1}$); open circles, PSI electron transfer rate (A-D) (ETR_{PSI}, $e^- \cdot s^{-1} \cdot PSI^{-1}$); gray circles, photochemical rate (E-H) (R_{PH}, $e^- \cdot s^{-1} \cdot PS^{-1}$); gray diamonds, PSI cyclic electron flow (J_{CEF}) calculated as follow: $J_{CEF} = ETR_{PSI} - ETR_{PSII}$ (see text for further information) (A-D) (J_{CEF}, $e^- \cdot s^{-1} \cdot PSI^{-1}$); grey diamonds, PSI cyclic electron flow (J_{CEF}) calculated as follow: $J_{CEF} = 2\ (R_{ph} - ETR_{PSII})$ (see text for further information) (E-H) (J_{CEF}, $e^- \cdot s^{-1} \cdot PSI^{-1}$). All measurements were performed at least in triplicate ($n \geq 3$) and data are presented as means ± SD.

197 conditions (*e.g.* in the presence of PSII inhibitor DCMU) (Johnson, 2011; Leister and Shikanai, 2013).
198 Two strategies are commonly accepted to provide physiological evidence for PSI-CEF activity: (i)
199 comparing electron transport rates of PSII (ETR_{PSII}) and PSI (ETR_{PSI}) (Harbinson et al., 1990) and (ii)
200 comparing electron transport rate of PSII (ETR_{PSII}) and mean photochemical rate based on ECS

measurement (R_{ph}) (Joliot and Joliot, 2002). In case of a pure linear electron flow, all enzyme complexes are expected to operate at the same rate. R_{ph}, ETR_{PSI}, and ETR_{PSII} should thus be equal in the absence of PSI-CEF and should follow the same temporal dependence. This is clearly the case in the *pgrl1* and *pgrl1 hydg-2* mutants (Figures 3B, 3D, 3F and 3H). On the contrary, an increase of R_{ph} and ETR_{PSI} (ETR_{PSII} remaining constant) reflected the onset of PSI-CEF in the wild type and *hydg-2* mutant within the first 200 seconds of illumination (Figures 3A, 3C, 3E and 3G). In order to quantify the contribution of PSI-CEF (J_{CEF} in $e^- \cdot s^{-1} \cdot PSI^{-1}$) to photosynthesis reactivation, we considered that PSI electron transfer rate is the sum of two components: $ETR_{PSI} = ETR_{PSII} + J_{CEF}$. Thus $J_{CEF} = ETR_{PSI} - ETR_{PSII}$ (Figures 3A-D). Given that ETR_{PSI} ($e^- \cdot s^{-1} \cdot PSI^{-1}$) + ETR_{PSII} ($e^- \cdot s^{-1} \cdot PSII^{-1}$) = 2 R_{ph} ($e^- \cdot s^{-1} \cdot PS^{-1}$) [which we confirmed experimentally (Supplemental Figure 4)], we can also write that $J_{CEF} = 2 (R_{ph} - ETR_{PSII})$ (Figures 3E-H). Again, those equations are valid if PSI/PSII ratio is 1 (see above and methods for further information). These two methods gave very similar estimations of PSI-CEF (Figure 3): J_{CEF} is null in the *pgrl1* and *pgrl1 hydg-2* mutants, whereas it increases during the first 200 seconds of illumination in wild type and *hydg-2* mutant before almost disappearing after ~5-6 minutes.

To our knowledge, these are the first measurements of PSI-CEF rate in physiological conditions (*i.e.* in the absence of inhibitors) in *C. reinhardtii*. The maximal rate for PSI-CEF achieved in wild type and *hydg-2* was 20 $e^- \cdot s^{-1} \cdot PSI^{-1}$, a rate corresponding to half the capacity of PGRL1-dependent PSI-CEF previously measured in high light in the presence of DCMU (Alric, 2014). PSI-CEF is induced in our conditions when LEF towards CBB cycle is still impaired due to a lack of ATP. When PSI-CEF reaches its maximal value after ~120 s of illumination (Figure 3), the PSI-CEF/LEF ratio (*i.e.* J_{CEF}/ETR_{PSII} ratio) is about 1.3 and 3.5 in wild type and *hydg-2,* respectively. Similarly, the PSI-CEF/LEF ratio also increased (up to four fold increase) when CBB cycle is impaired due to carbon limitation in oxic conditions (Lucker and Kramer, 2013). These finding are in good agreement with the proposal that PSI-CEF contributes to adjust the ATP/NADPH ratio for photosynthetic carbon fixation in various energetic unfavourable conditions (Allen, 2003). In anoxia, both PQ and PSI acceptor pools are almost fully reduced (Bennoun, 1982; Ghysels et al., 2013; Takahashi et al., 2013; Godaux et al., 2013), which might hamper the putative limiting step of PSI-CEF electron transfer (i.e. NADPH to PQ; (Alric, 2014), as well as the PSI electron transfer due to acceptor side limitation (Takahashi et al., 2013). It is tempting to propose that hydrogenase activity, by partially reoxidizing the PQ pool and FDX, might directly contribute to set the redox poise allowing the PSI-CEF to operate. However, the fact that PSI-CEF operate at the same rate in wild type and *hydg-2* (Figure 3) suggests that another factor might be responsible for its activation.

Reduction of the PQ pool also triggers state transitions, a process consisting in the phosphorylation and migration of part of light harvesting complexes (LHC) II from photosystem (PS) II

to PSI (reviewed in (Lemeille and Rochaix, 2010)). Since State 2 facilitates induction of PSII activity in the absence of hydrogenase (Ghysels et al., 2013), we propose that the increase of PSI antenna size upon state 2 might enhance PSI-CEF rate (as earlier suggested in (Cardol et al., 2009; Alric, 2010; Alric, 2014)), and therefore promote ATP synthesis and CBB cycle activity. Nevertheless, the attachment of LHC-II to PSI in state 2 has been recently called into question (Unlu et al., 2014; Nagy et al., 2014). In this respect, the involvement of state transitions could be to decrease PSII-reductive pressure on PQ pool that might impact PSI-CEF rate (see above). In any cases, the transition from State 2 to State 1 did not seem to occur in our range of time as there was no major change in the Fm' value (Supplemental Figure 5). Incidentally, our measurements of a transient PSI-CEF under state II provide the first *in vivo* support to the occurrence of PSI-CEF without any direct correlation with state transitions (Takahashi et al., 2013; Alric, 2014).

Sequential and transient hydrogenase activity and PSI-CEF contribute to photosynthetic carbon fixation.

At this point, we can conclude that the CBB cycle is progressively active in wild type thanks to the sequential occurrence of HYDA-dependent LEF and PGRL1-dependent PSI-CEF. This is further illustrated in a schematic model of electron transfer pathways in wild type (Figure 4A). At the onset of illumination, only a hydrogenase-dependent LEF occurs (10 seconds), followed by the induction of PGRL1-dependent PSI-CEF and later CBB cycle (120 to 240 seconds). When CBB cycle has been activated by ATP, $NADP^+$ pool is partially oxidized and FNR, being more efficient in competing for reduced FDX than hydrogenases (see next section) (Yacoby et al., 2011), drives rapidly the entire electron flux towards CO_2 reduction (> 360 seconds). In single mutants, increase in CBB cycle activity is only slightly delayed (Figures 4B and 4C) while lack of both AEF fully prevents photosynthetic electron transfer in *pgrl1 hydg-2* double mutant (Figure 4D).

ETR did not exceed 5 $e^- \cdot s^{-1} \cdot PSI^{-1}$ in *pgrl1 hydg-2* double mutant, and might correspond to a NDA2-driven ETR (Jans et al., 2008; Alric, 2014). The low rate measured here is in good agreement with the rate of 2 $e^- \cdot s^{-1} \cdot PSI^{-1}$measured for PQ reduction by NDA2 (Houille-Vernes et al., 2011) and the rate of 50-100 nmoles $H_2 \cdot$ mg chlorophyll $^{-1} \cdot min^{-1}$ determined for NDA2-driven H_2 production

262 from starch degradation (Baltz et al., 2014), the latter value also corresponding to ~1-2 $e^- \cdot s^{-1} \cdot PSI^{-1}$,
263 assuming 500 chlorophyll per photosynthetic unit (Kolber and Falkowski, 1993). Alternatively this
264 remaining ETR in the double mutant might correspond to the activity of another chloroplastic
265 fermentative pathways linked to ferredoxin reoxidation (Grossman et al., 2011). Regarding these

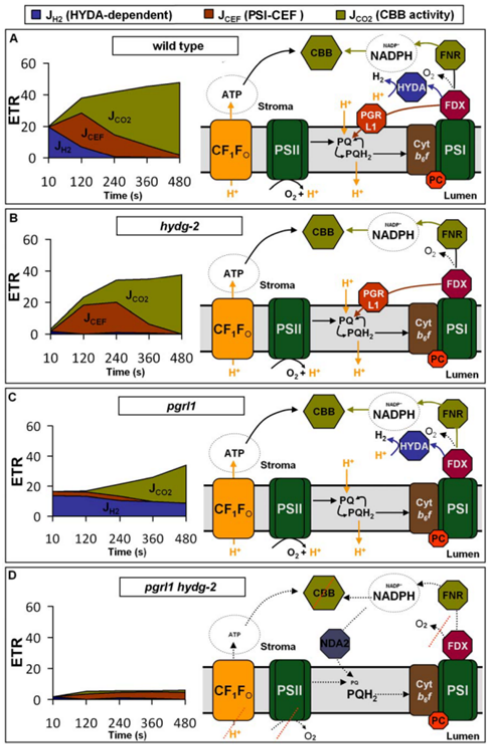

Figure 4. Schematic model of photosynthetic electron transfers (ETR) in *C. reinhardtii* upon a shift from dark-anoxia (1 hour) to light in wild type (A), *hydg-2* (B), *pgrl1* (C), and *pgrl1 hydg-2* (D). PSI-CEF (J_{CEF}), hydrogen evolution rate (J_{H2}), and electron transport rate towards CO2 fixation (J_{CO2}) refer to electron rates ($e^- \cdot s^{-1} \cdot PSI^{-1}$) taken from Figures 1 and 3. FDX, ferredoxin; HYDA, hydrogenase; FNR, ferredoxin-NADP$^+$ oxidoreductase; PGRL1, proton-gradient regulation like1 protein; NDA2, type II NAD(P)H dehydrogenases; PC, plastocyanin; Cyt b_6f, cytochrome b_6f complex; CBB, Calvin-Benson-Bassham cycle; PQ/PQH_2, plastoquinone pool; PSI and PSII, photosystems I and II; CF_1F_O, chloroplastic ATP synthase.

possibilities, we ensured that the starch content of wild types and mutants before entering anoxia does not differ between mutants and their respective wild type (Table 1). Whatever the exact nature of the remaining ETR in *pgrl1 hydg-2*, these results confirm that at least one of the two AEF (PSI-CEF or hydrogenase-dependent LEF) is necessary for the proper induction of PSII activity in anoxia.

Since the absence of significant ETR in *pgrl1 hydg-2* applies for a given period of incubation in the dark in anoxia (1 hour) and for a given light intensity (250 µmol photons · m^{-2} · s^{-1}), we explored induction of PSII electron transfer (i) during a longer illumination period (up to 2 hours) (Supplemental Figure 6), (ii) after shorter (10 minutes) or longer (16 hours) periods of anoxia in the dark (Figures 5A and 5B), and (iii) upon lower and higher light intensities (120 and 1,000 µmol photons . m^{-2} . s^{-1}, respectively) (Figures 5C and 5D). In every condition, photosynthetic electron flow of the double mutant remained null or very low compared to the wild-type and single mutant strains. The only exception to this rule is the low ETR in *pgrl1* after 10 minutes of anoxia (Figure 5A), which is probably be due to the fact the hydrogenases are not yet fully expressed (Forestier et al., 2003; Pape et al., 2012), and therefore mimics the behavior of *pgrl1 hydg-2*.

Competition between FNR and HYDA contributes to the observed decreased in hydrogen evolution rate.

O_2 sensitivity of algal hydrogenases is defined as the major challenge to achieve a sustained hydrogen photoproduction. Hydrogenases are described as irreversibly inactivated after exposure to O_2, the *C. reinhardtii* enzyme being the most O_2-sensitive among them (Cohen et al., 2005; Ghirardi et al., 1997). In the PGRL1-deficient mutant or in the presence of GA or CCCP (*i.e.* in the absence of CO_2 fixation), we observed however a sustained hydrogen evolution rate (J_{H2}) lasting for at least ten minutes after transfer to light (Figures 1B, 2A, 2B, 2E and 2F), and coexisting with a significant PSII activity and thus a sustained production of oxygen by water splitting. A possible explanation for this long lasting hydrogen production is that we used in these experiments glucose and glucose oxidase which efficiently reduces oxygen evolved by PSII and diffusing to the extracellular medium. We thus performed a similar experiment as presented in Figure 1 for wild type and *pgrl1* mutant cells where anoxia was reached by bubbling nitrogen for 5 minutes and cells were then acclimated to dark and anoxia for 1 hour. In wild type, hydrogen evolution stops while level of dissolved oxygen is still low in the medium (~10 µM) (Figure 6A). Conversely, in *pgrl1*, a sustained hydrogen evolution occurs in the presence of much higher concentrations of dissolved oxygen (up to ~80 µM) (Figure 6B). This leads us to suggest that *in vivo* oxygen-sensitivity of hydrogenase activity is not the only factor that accounts for the decrease of J_{H2} in the light in wild type. It was proposed earlier that the slow-down of the hydrogenase activity in wild-type cells stems from a thermodynamic break (Tolleter et al., 2011). In this view, the PSI-CEF would generate an extra proton gradient that would slow-down the cytochrome b_6f and therefore decrease the electron supply from PSII to the hydrogenase. This seems very unlikely since PSII activity (ETR_{PSII}) and photosynthetic carbon fixation (J_{CO2}) tends to increase while hydrogen activity (J_{H2}) decreases (Figure 1). In addition, H_2 evolution rate is about the same in

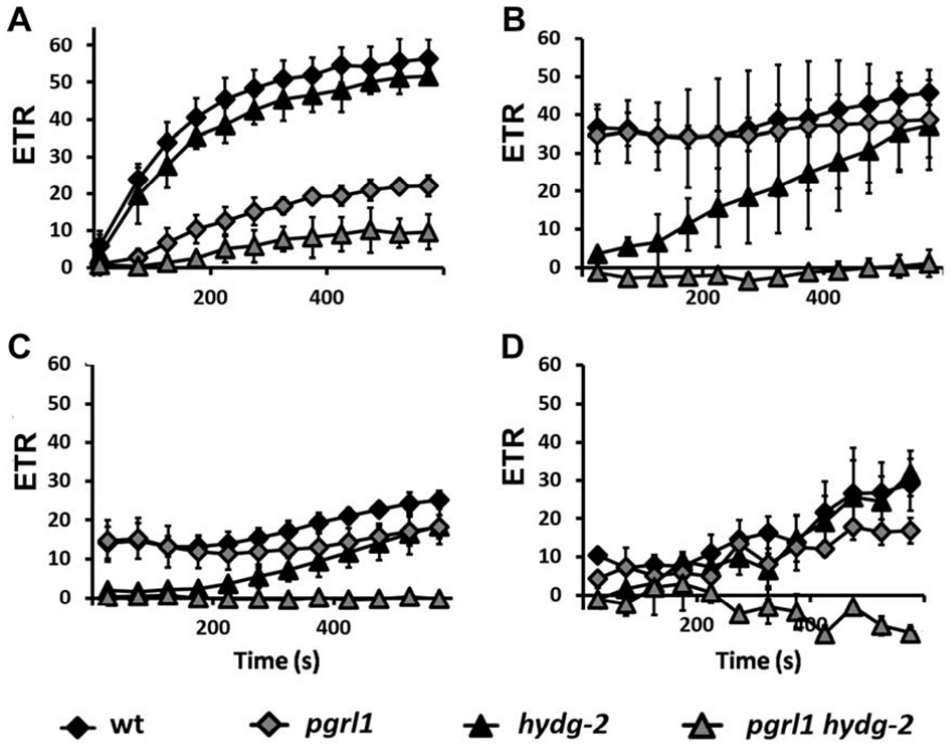

Figure 5. **PSII electron transfer rate** (ETR_{PSII}, $e^- \cdot s^{-1} \cdot PSII^{-1}$) in wild type, *pgrl1*, *hydg-2* and *pgrl1 hydg-2* (A) upon a shift from dark anoxia (10 minutes) to light (250 µmol photons $\cdot m^{-2} \cdot s^{-1}$); (B) upon a shift from dark anoxia (16 hours) to light (250 µmol photons $\cdot m^{-2} \cdot s^{-1}$); (C) upon a shift from dark anoxia (1 hour) to light (120 µmol photons $\cdot m^{-2} \cdot s^{-1}$); (D) upon a shift from dark anoxia (1 hour) to light (1,000 µmol photons $\cdot m^{-2} \cdot s^{-1}$). All measurements were performed at least in triplicate ($n \geq 3$) and data are presented as means ± SD.

1

304 presence of either a proton gradient uncoupler (CCCP) or a CCB cycle inhibitor (GA) (Figure 2), whose
305 presence should decrease and increase the amplitude of the proton gradient, respectively. In this
306 respect, it was recently shown that NADPH reduction by FNR prevents an efficient H_2 production by
307 HYDA *in vitro* (Yacoby et al., 2011). This might be due to the low affinity of HYDA for FDX (K_M = 35

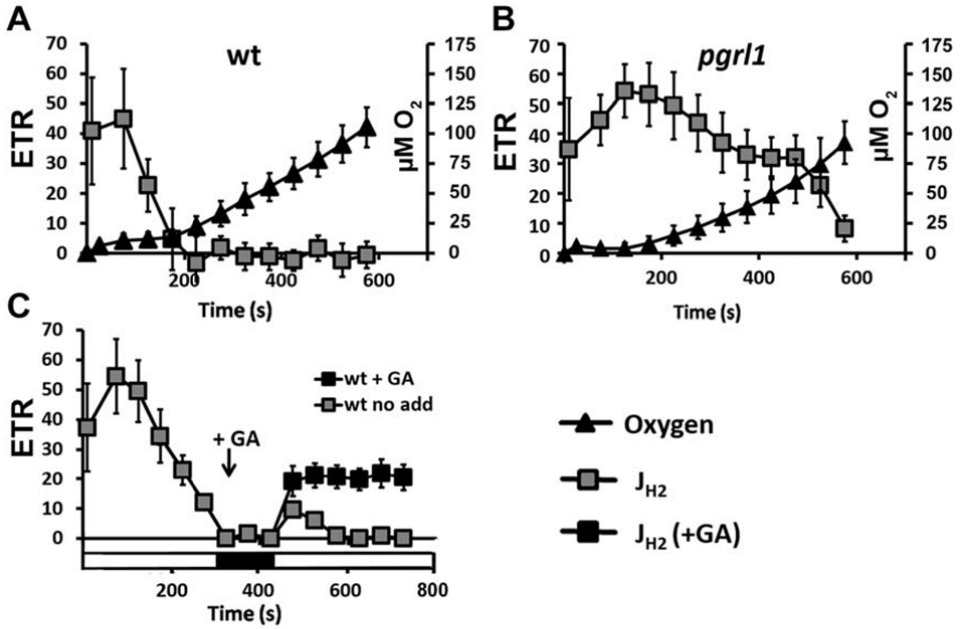

Figure 6. *In vivo* hydrogenase activity. (A-B) Concomitant measurements of hydrogen evolution rate (grey squares, J_{H2}, $e^- \cdot s^{-1} \cdot PSI^{-1}$) and dissolved oxygen concentration (dark triangles, μMO_2) in (A) wild type and (B) *pgrl1* upon a shift from dark anoxia (1 hour) to light. Anoxia was reached by bubbling with nitrogen for 5 minutes prior incubation in the dark for 1 hour. (C) Hydrogen evolution rate (J_{H2}, $e^- \cdot s^{-1} \cdot PSI^{-1}$) upon a shift from dark anoxia (1 hour) to light. Arrow, when hydrogen evolution stops, CBB activity is inhibited by addition of glycolaldehyde (GA, 10mM, dark squares). After 2 minutes of incubation in the dark, light is switched on for at least 6 extra minutes. All measurements were performed at least in triplicate (n ≥ 3) and data are presented as means ± SD.

1

µM; (Happe and Naber, 1993), close to 2 orders of magnitude lower than the affinity of FNR for FDX (K_M = 0.4 µM; (Jacquot et al., 1997)). To test whether competition between FNR and HYDA might contribute to decrease in J_{H2} *in vivo* in wild type, we tested the effect of the addition of GA (inhibitor of CCB cycle) on wild-type cells when J_{H2} was null (*i.e.* after few minutes of illumination). If

hydrogenase was indeed irreversibly inactivated by oxygen, J_{H2} should remain null whatever the inhibition of CBB cycle activity. Yet, upon addition of GA, J_{H2} again increases while it remains null in the absence of GA (Figure 6C). We thus propose that the competition between HYDA and FNR for reduced ferredoxin is an important factor responsible for the switch in electron transfer from hydrogenase activity (J_{H2}) towards CBB cycle activity (J_{CO2}) (Figure 1). In agreement with this, transformants displaying reduced Photosynthesis/Respiration (P/R) ratio reach anoxia in the light, express hydrogenase but evolve only small amount of H_2 *in vivo* unless Calvin cycle is inhibited (Ruhle et al., 2008).

PSII activity, besides supplying hydrogenases and CBB cycle activity in electrons, produces oxygen by water splitting. Various oxidases, such as the mitochondrial cytochrome *c* oxidase, might contribute to cellular ATP synthesis and in turn to CBB cycle activity by using oxygen as electron acceptor (Lavergne, 1989). In this respect, recent works have highlighted the dependence of PSI-CEF deficient mutants upon oxygen in *Chlamydomonas* and *Arabidopsis*, through an increase of mitochondrial respiration and PSI-Mehler reaction (Yoshida et al., 2011; Johnson et al., 2014; Dang et al., 2014). Regarding contribution of respiration to induction of photosynthetic electron flow in anoxia, the addition of myxothiazol, an efficient inhibitor of mitochondrial respiratory-chain cytochrome bc_1 complex (complex III) prior illumination (Supplemental Figure 7) has no effect. As shown in Figure 2A, the addition of GA fully prevents the increase of photosynthetic electron flow, which is almost exclusively driven under these conditions by hydrogenase. This indicates that, if occurring, other alternative processes (*e.g.* Mehler reaction) operate at a very low rate.

Concomitant absence of hydrogenase activity and PGRL1-dependent PSI-CEF is detrimental for cell survival.

Photosynthesis relies on a large set of alternative electron transfer pathways allowing the cells to face various changes of environmental conditions. Deficiency in some pathways can be successfully compensated by other pathways (e.g. (Dang et al., 2014; Cardol et al., 2009)). To check whether the lack of hydrogenase activity and/or PSI-CEF has an impact on the growth of *C. reinhardtii* in anoxia, the four strains were grown individually and submitted to 3h dark/3h light cycles in sealed cuvettes. This time scale was chosen (i) to ensure that anoxia is reached during dark cycle so that hydrogenase is expressed in wild type and in *pgrl1*, and (ii) to maximize the impact of mutations that impair photosynthesis reactivation steps. The doubling time of *pgrl1 hydg-2* cells in anoxia was much lower compared to wild-type and single mutant cells (Figure 7A). In a second experiment, wild-type and *pgrl1 hydg-2* double mutant cells were mixed in equal proportion and submitted to the same growth test. The ratio between *pgrl1 hydg-2* mutant and wild-type cells progressively decreased and

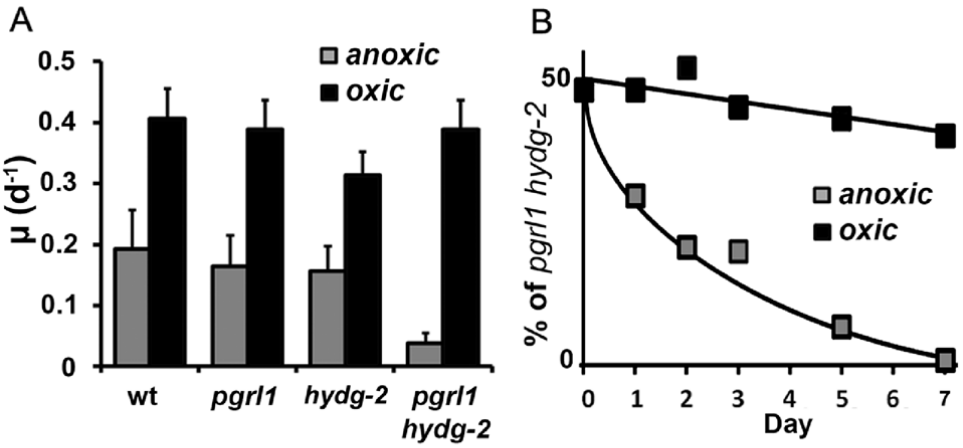

Figure 7. Growth in anoxic conditions. (A) Specific growth rate (μ, day^{-1}) of wild type and mutants in 3h dark/3h light cycles in TMP liquid medium. (B) Proportion of *pgrl1 hydg-2* mutant within a co-culture of *pgrl1 hydg-2* and wild-type cells in 3h dark/3h light cycle in TAP liquid medium (see material and method section for further details). Dark squares, aerated culture; grey squares, anoxic sealed culture. All measurements were performed at least in triplicate (n ≥ 3) and data are presented as means ± SD.

only wild-type cells were recovered after 7 days of growth in sealed cuvettes under anoxic conditions (Figure 7B). PGRL1-dependent PSI-CEF has been proposed to be crucial for acclimation and survival in anoxic conditions under a constant light regime, both in *Physcomitrella* and *Chlamydomonas* (Kukuczka et al., 2014). In our experimental conditions, growth of *pgrl1* mutant was not impaired

(Figure 7A) and Calvin cycle reactivation only slightly delayed (Figures 1B and 4C). We attribute this phenotype to hydrogenase activity that could play in anoxia the same role as the Mehler reaction in the presence of oxygen. Simultaneous absence of hydrogenase activity and PGRL1-dependent PSI-CEF however fully prevents the induction of photosynthetic electron flow (Figures 1D and 4D) and in turn growth (Figure 7). Our results thus highlight the importance for *C. reinhardtii* of maintaining at least hydrogenase activity or PSI-CEF to survive in its natural habitat where it frequently encounters oxygen limitation.

MATERIALS AND METHODS

Strains. *C. reinhardtii* wild-type strain (*1'* in our stock collection) derives from *137c* reference wild-type strain. The *hydg-2* mutant lacking the HYDG maturation factor and deficient for hydrogenase (HYDA enzyme) was obtained in our laboratory from insertional mutagenesis carried out on *1'* strain (Godaux et al., 2013). An allelic *hydg-3* mutant strain was also tested and displayed the same features (data not shown). The *pgrl1* mutant defective in PSI-CEF was generated by insertional mutagenesis carried out on *137c* (Tolleter et al., 2011). The wild-type strain from which derived the single *pgrl1* mutant, and the complemented strain for *PGRL1* (Tolleter et al., 2011) did not differ from wild-type 1' strain (Table 1 and 2). The double mutant *pgrl1 hydg-2* was obtained by crossing the *pgrl1 mt*$^{-}$ mutant with the *hydg-2 mt+* mutant (see Supplemental Figure 1 for details).

Strains were routinely grown in Tris-Acetate-Phosphate (TAP) or eventually on Tris-Minimal-Phosphate (TMP) medium at 25°C under continuous light of 50 µmol photons · m^{-2} · s^{-1} either on solid (1.5 % agar) or in liquid medium. For experimentation, cells were harvested (3,000 *g* for 2 minutes) during exponential growth phase (2-4.10^{6} cells · ml^{-1}) and re-suspended in fresh TAP medium at a concentration of 10 µg chlorophyll · ml^{-1}. 10 % (w/v) Ficoll was added to prevent cell sedimentation during spectroscopic analysis.

Chlorophyll and starch contents. For the determination of chlorophyll concentration, pigments were extracted from whole cells in 90 % methanol and debris were removed by centrifugation at 10,000 *g*. Chlorophyll a + b concentration was determined with a lambda 20 spectrophotometer (Perkin Elmer, Norwalk, CT). Starch was extracted according to (Ral et al., 2006). Starch amounts were determined spectrophotometrically using the Starch Kit, Roche, R-Biopharm.

Biophysical analyses. In all experiments cells were acclimated to dark and anoxia for one hour before transfer to light. Unless otherwise stated, anoxic condition was reached by sealing cell suspension in spectrophotometric cuvettes in the presence of catalase (1000 U · ml^{-1}), glucose (10 mM), and glucose oxidase (2 mg · ml^{-1}).

In vivo chlorophyll fluorescence measurements were performed at room temperature on cell liquid suspensions using a JTS-10 spectrophotometer (Biologic, France). In most experiments, an actinic light of 250 µmol photons · m^{-2} · s^{-1} was provided by a 640-nm LED light sources. This light intensity corresponds to ~100 e^- · s^{-1} · $PSII^{-1}$ in oxic conditions (Table 1). The effective photochemical yield of Photosystem II (Φ_{PSII}) was calculated as (F_M'-F_S)/F_M', where F_S is the actual fluorescence level excited by actinic light and F_M' is the maximum fluorescence emission level induced by a 150 ms superimposed pulse of saturating light (3,500 µmol photons · m^{-2} · s^{-1}).

P_{700} absorption changes were assessed with a probing light peaking at 705-nm. Actinic light of 250 µmol photons · m^{-2} · s^{-1} was provided by a 640-nm LED light sources, which was switched off very briefly while measuring light transmission at 705-nm. In order to remove unspecific contributions to the signal at 705-nm, absorption changes measured at 740-nm were subtracted. The quantum yield of photochemical energy conversion by PSI (Φ_{PSI}) was calculated as (P_M'–P_S)/(P_M-P_0) (Klughammer and Schreiber, 2008). P_0 is the absorption level when P_{700} are fully reduced, P_M is the absorption level when P_{700} are fully oxidized in presence of 20 µM DCMU and 5 mM DBMIB (to prevent P_{700} rereduction by cytochrome *b_6f* complex activity) upon saturating continuous illumination, P_S is the absorbance level under continuous illumination and P_M' is the maximal absorption level reached during a 200 ms saturating light pulse (3,500 µmol photons · m^{-2} · s^{-1}) on top of the actinic light. P_{700} concentration was estimated by using P_M value (ε705nm for P_{700} = 105 mM^{-1} cm^{-1}; (Witt et al., 2003)).

ECS analyses. The generation of an electrochemical proton gradient induces a shift in the absorption spectra of some photosynthetic pigments, resulting in the so-called ElectroChromic Shift. The use of the ECS signal to study photosynthetic apparatus and a detailed description of the different application is reviewed in (Bailleul et al., 2010). The relaxation kinetics of the carotenoid electrochromic bandshift was measured at 520-nm and corrected by subtracting the signal at 546-nm. Photochemical rates (R_{ph}) were measured by following the relaxation of the ECS during the first 2 ms after switching off the actinic light (Joliot and Joliot, 2002). Results were expressed as e^- · s^{-1} · PS^{-1} upon normalization to the amplitude of ECS signal upon excitation with a saturating flash (5 ns laser pulse) that lead to one single charge separation per PS (Bailleul et al., 2010).

In this report, we calculated photosynthetic electron flows assuming that PSI/PSII stoichiometry is about 1 in all our strains. Doing so, we attempted to simplify calculations and make the study accessible for non-specialists. The ratio between active PSI and PSII centers was however estimated as described in (Cardol et al., 2009). Briefly, the amplitude of the fast phase (1 ms) of ECS signal (at 520-546-nm) was monitored upon excitation with a laser flash. The contribution of PSII was calculated from the decrease in the ECS amplitude after the flash upon the addition of the PSII

414 inhibitors DCMU (20 µM) and HA (1 mM), whereas the contribution of PSI corresponded to the
415 amplitude of the ECS that was insensitive to these inhibitors.

416 When taking into account PSI/PSII stoichiometry measured in Table 1, J_{CO2} can be calculated
417 according the following equation: $J_{CO2} = ETR_{PSII} * (1/b) – J_{H2}$, where b is the ration between PSI and
418 PSII active centers. Similarly, $J_{CEF} = ETR_{PSI} – ETR_{PSII} * (1/b)$ and $J_{CEF} = (1+b) * (R_{ph} – ETR_{PSII}) / b$. R_{ph}
419 calculated in this manner is equal to half the sum of ETR_{PSI} and ETR_{PSII} when PSI/PSII stoichiometry is
420 about 1 (Supplemental Figure 4). For wild type 1', that has the largest PSI/PSII ratio (Table 1),
421 photosynthetic electron flows are modified at most by 15%.

422 The calculation of ETR_{PSI} and ETR_{PSII} usually also requires the quantification of the absorption
423 cross sections of PSII (σ_{PSII}) and PSI (σ_{PSI}), which can change with time through the process of state
424 transitions (Alric, 2014; Wollman and Delepelaire, 1984). However, we could show that the PSII cross
425 sections did not change in our conditions by monitoring Fm' (Supplemental Figure 5). Moreover only
426 a hydrogenase-dependent LEF occurs at the onset of light, which allowed us to use the
427 photochemical rates measured by ECS, fluorescence and P_{700} at the initial onset of light as a ruler to
428 determine ETR_{PSI} and ETR_{PSII} based on the sole PS quantum yields measurements. At the onset of
429 light, $\phi_{PSII} = 0.12$ and $\phi_{PSI} = 0.21$ (Table 2). This leads to $ETR_{PSII}(t=0) = \phi_{PSII} \cdot I \cdot \sigma_{PSII} = 20\ e^- \cdot s^{-1} \cdot PSII^{-1}$
430 and to $ETR_{PSI}(t=0) = \phi_{PSI} \cdot I \cdot \sigma_{PSI} = 20\ e^- \cdot s^{-1} \cdot PSI^{-1}$, where I is the actinic light intensity. We therefore
431 calculated ETR_{PSII} ($e^- \cdot s^{-1} \cdot PSII^{-1}$) as $(20/0.12) \cdot \phi_{PSII}$ and ETR_{PSI} ($e^- \cdot s^{-1} \cdot PSI^{-1}$) as $(20/0.21) \cdot \phi_{PSI}$.

432 Oxygen and hydrogen exchange rates were measured at 25°C using an oxygen-sensitive Clark
433 electrode (Oxygraph, Hansatech Instruments), eventually modified to only detect hydrogen (Oxy-Ecu,
434 Hansatech Instruments). Actinic light was provided by a home-made light system composed of white
435 and green LEDs. Oxygen solubility in water is about 258 µM at 25°C. For hydrogen evolution
436 measurements (nmoles $H_2 \cdot$ µg $chloro^{-1} \cdot s^{-1}$), the entire set-up was placed in a plastic tent under
437 anoxic atmosphere (N_2) to avoid contamination of anoxic samples by oxygen while filling the
438 measuring cell. Hydrogen evolution rates (J_{H2}) were calculated on the basis of first derivative of
439 hydrogen production curves (data not shown) and expressed in $e^- \cdot s^{-1} \cdot PSI^{-1}$ according to the
440 following calculation: (nmoles $H_2 \cdot$ µg $chloro^{-1} \cdot s^{-1}$) $\cdot 2 \cdot$ (µg chloro $\cdot$ pmoles P_{700}), assuming 2 e^- per H_2
441 evolved.

442 **<u>Growth experiments</u>**. Doubling time at 250 µmol photons $\cdot m^{-2} \cdot s^{-1}$ in TMP medium was
443 determined from DO_{750nm}, cell number and chlorophyll content (initial cell density of 2.10^5-10^6 cells $\cdot$
444 ml^{-1}). We did not investigated higher light intensities because the PGRL1-defective strains are high-
445 light sensitive (Dang et al., 2014; Tolleter et al., 2011).

Wild-type and *pgrl1 hydg-2* strains were mixed together at equal concentration of 5.10^5 cells $\cdot$ ml^{-1} in fresh TAP medium. Aliquots of the liquid culture were then collected every 24 hours and about 300 cells were platted on solid TAP media in the light to allow the growth of single-cell colonies. The proportions of each phenotype were analyzed on the basis of peculiar hydrogenase-deficient related chlorophyll fluorescence kinetic by video-imaging according to (Godaux et al., 2013). Ratio of *pgrl1 hydg-2* was plotted against time.

During growth experiments in anoxia, catalase (1000 U $\cdot$ mL^{-1}), glucose (10 mM), and glucose oxidase (2 mg $\cdot$ mL^{-1}) were added at the beginning of the experiment. Glucose (10mM) was subsequently added every 24 hours to ensure that glucose oxidase consume oxygen evolved during the light periods, so that oxygen did not inhibit hydrogenase expression.

Acknowledgements.

René Matagne is warmly acknowledged for careful reading of the manuscript and help in genetics experiments. We also thank C. Remacle, F. Franck and F. Rappaport for their critical comments during the preparation of this manuscript. PC acknowledged financial support from the Belgian Fonds de la Recherche Scientifique F.R.S.-F.N.R.S. (F.R.F.C. 2.4597.11, CDR J.0032.15 and Incentive Grant for Scientific Research F.4520) and University of Liège (SFRD-11/05). DG is supported by the Belgian FRIA F.R.S.-FNRS. BB and PC are Short Term Foreign Postdoctoral Fellow and Research Associate from F.R.S.-FNRS, respectively.

Author Contributions. DG, BB, PC designed the research and wrote the paper; DG, BB, NB, PC performed research and analyzed data.

Figure Legends

Figure 1. Activities of PSII, hydrogenases and CBB upon a shift from dark-anoxia (1 hour) to light (250 µmol photons $\cdot$ m^{-2} $\cdot$ s^{-1}) in wild type (*A*), *pgrl1* (*B*), *hydg-2* (*C*), and *pgrl1 hydg-2* (*D*). **ETR**, electron transport rate. Dark circles, PSII electron transfer rate (ETR_{PSII}, e^- $\cdot$ s^{-1} $\cdot$ $PSII^{-1}$); grey squares, hydrogen evolution rate (J_{H2}, e^- $\cdot$ s^{-1} $\cdot$ PSI^{-1}); open triangle, electron flow towards carbon fixation (J_{CO2}, e^- $\cdot$ s^{-1} $\cdot$ PSI^{-1}) calculated as follow: $J_{CO2} = ETR_{PSII} - J_{H2}$ (see text for further information). All measurements were performed at least in triplicate ($n \geq 3$) and data are presented as means ± SD.

Figure 2. Activities of PSII, hydrogenases and CBB upon a shift from dark-anoxia (1 hour) to light (250 µmol photons · m^{-2} · s^{-1}) in wild type (A, B), *hydg-2* (C, D) and *pgrl1* (E, F) in conditions of inhibition of the CBB cycle. Glycolaldehyde (GA, 10mM) (*A*, *C*, *E*), or carbonyl cyanide m-chlorophenyl hydrazone (CCCP, 20µM) (*B*, *D*, *F*) were added prior illumination. **ETR**, electron transport rate. Dark circles, PSII electron transfer rate (ETR_{PSII}, e^- · s^{-1} · $PSII^{-1}$); gray squares, hydrogen evolution rate (J_{H2}, e^- · s^{-1} · PSI^{-1}); open triangle, electron flow towards carbon fixation (J_{CO2}, e^- · s^{-1} · PSI^{-1}) calculated as follow: $J_{CO2} = ETR_{PSII} - J_{H2}$ (see text for further information). All measurements were performed at least in triplicate (n ≥ 3) and data are presented as means ± SD.

Figure 3. PSI cyclic electron flow upon a shift from dark-anoxia (1 hour) to light in wild type (A, E), *pgrl1* (B, F), *hydg-2* (C, G) and *pgrl1 hydg-2* (D, H). **ETR**, electron transport rate. Dark circles, PSII electron transfer rate (A-H) (ETR_{PSII}, e^- · s^{-1} · $PSII^{-1}$); open circles, PSI electron transfer rate (A-D) (ETR_{PSI}, e^- · s^{-1} · PSI^{-1}); gray circles, photochemical rate (E-H) (R_{PH}, e^- · s^{-1} · PS^{-1}); gray diamonds, PSI cyclic electron flow (J_{CEF}) calculated as follow: $J_{CEF} = ETR_{PSI} - ETR_{PSII}$ (see text for further information) (A-D) (J_{CEF}, e^- · s^{-1} · PSI^{-1}); grey diamonds, PSI cyclic electron flow (J_{CEF}) calculated as follow: $J_{CEF} = 2$ (R_{ph} – ETR_{PSII}) (see text for further information) (E-H) (J_{CEF}, e^- · s^{-1} · PSI^{-1}). All measurements were performed at least in triplicate (n ≥ 3) and data are presented as means ± SD.

Figure 4. Schematic model of photosynthetic electron transfers (ETR) in *C. reinhardtii* upon a shift from dark-anoxia (1 hour) to light in wild type (A), *hydg-2* (B), *pgrl1* (C), and *pgrl1 hydg-2* (D). PSI-CEF (J_{CEF}), hydrogen evolution rate (J_{H2}), and electron transport rate towards CO2 fixation (J_{CO2}) refer to electron rates (e^- · s^{-1} · PSI^{-1}) taken from Figures 1 and 3. FDX, ferredoxin; HYDA, hydrogenase; FNR, ferredoxin-$NADP^+$ oxidoreductase; PGRL1, proton-gradient regulation like1 protein; NDA2, type II NAD(P)H dehydrogenases; PC, plastocyanin; Cyt b_6f, cytochrome b_6f complex; CBB, Calvin-Benson-Bassham cycle; PQ/PQH_2, plastoquinone pool; PSI and PSII, photosystems I and II; CF_1F_0, chloroplastic ATP synthase.

Figure 5. **PSII electron transfer rate** (ETR_{PSII}, e^- · s^{-1} · $PSII^{-1}$) in wild type, *pgrl1*, *hydg-2* and *pgrl1 hydg-2* (A) upon a shift from dark anoxia (10 minutes) to light (250 µmol photons · m^{-2} · s^{-1}); (B) upon a shift from dark anoxia (16 hours) to light (250 µmol photons · m^{-2} · s^{-1}); (C) upon a shift from dark anoxia (1 hour) to light (120 µmol photons · m^{-2} · s^{-1}); (D) upon a shift from dark anoxia (1 hour) to light (1,000 µmol photons · m^{-2} · s^{-1}). All measurements were performed at least in triplicate (n ≥ 3) and data are presented as means ± SD.

Figure 6. *In vivo* hydrogenase activity. (A-B) Concomitant measurements of hydrogen evolution rate (grey squares, J_{H2}, $e^- \cdot s^{-1} \cdot PSI^{-1}$) and dissolved oxygen concentration (dark triangles, μMO_2) in (A) wild type and (B) *pgrl1* upon a shift from dark anoxia (1 hour) to light. Anoxia was reached by bubbling with nitrogen for 5 minutes prior incubation in the dark for 1 hour. (C) Hydrogen evolution rate (J_{H2}, $e^- \cdot s^{-1} \cdot PSI^{-1}$) upon a shift from dark anoxia (1 hour) to light. Arrow, when hydrogen evolution stops, CBB activity is inhibited by addition of glycolaldehyde (GA, 10mM, dark squares). After 2 minutes of incubation in the dark, light is switched on for at least 6 extra minutes. All measurements were performed at least in triplicate ($n \geq 3$) and data are presented as means ± SD.

Figure 7. Growth in anoxic conditions. (A) Specific growth rate (μ, day^{-1}) of wild type and mutants in 3h dark/3h light cycles in TMP liquid medium. (B) Proportion of *pgrl1 hydg-2* mutant within a co-culture of *pgrl1 hydg-2* and wild-type cells in 3h dark/3h light cycle in TAP liquid medium (see material and method section for further details). Dark squares, aerated culture; grey squares, anoxic sealed culture. All measurements were performed at least in triplicate ($n \geq 3$) and data are presented as means ± SD.

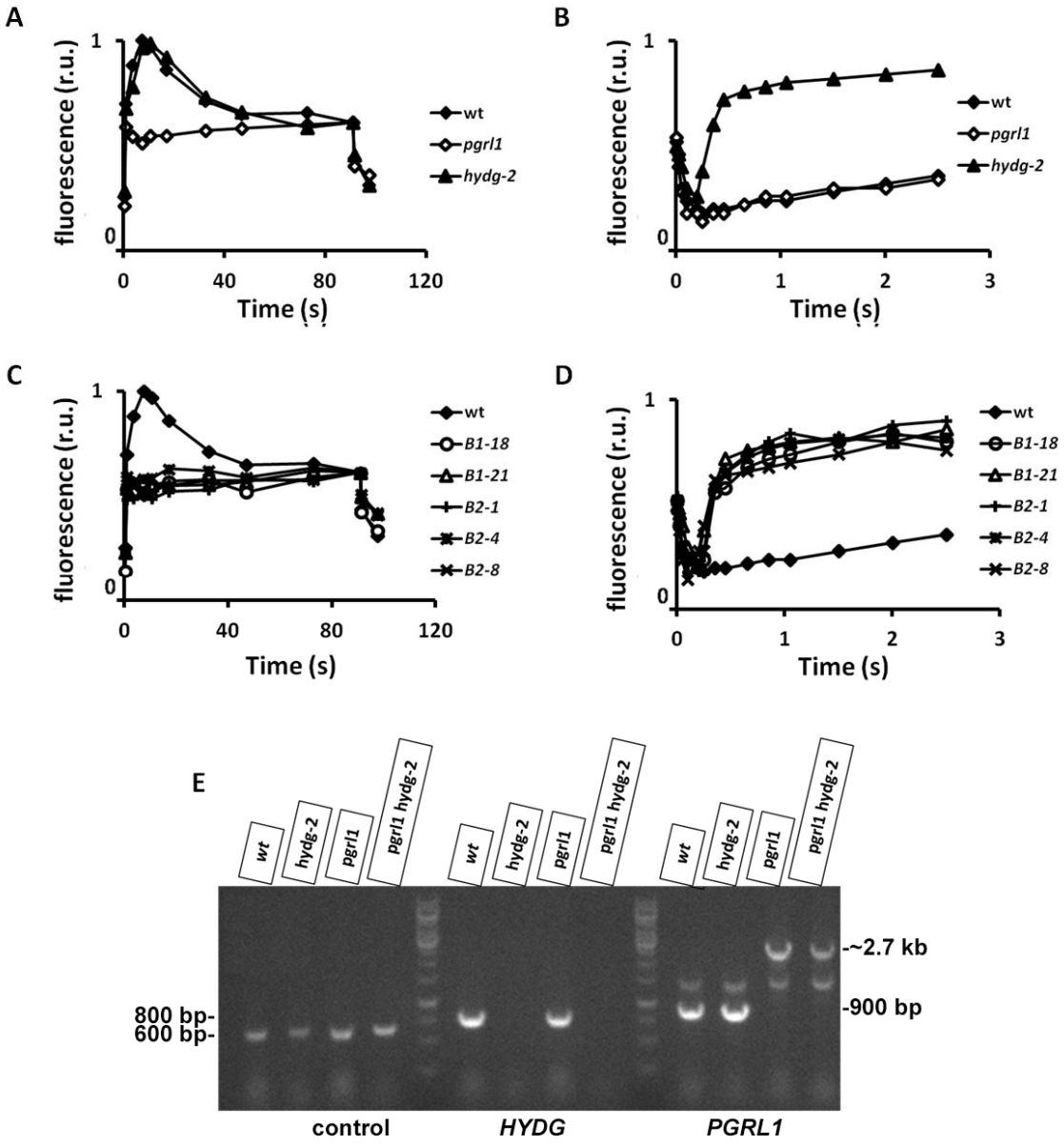

Supplemental Figure 1. **Isolation of *pgrl1 hydg*-2 double mutants by a double chlorophyll fluorescence screen**. Double mutant *pgrl1 hydg-2* were obtained by crossing the *pgrl1 mt*⁻ mutant with the *hydg-2 mt+* mutant and meiotic progeny was selected on TAP medium containing 25 mg/l hygromycin-B and 10 mg/l paromomycin. Both parental strains have been isolated on the basis of peculiar chlorophyll fluorescence kinetics, respectively in oxic conditions for *pgrl1* (*A*) (1) and in anoxic conditions for *hydg-2* (B) (2). Out of 78 meiotic products screened for both specific fluorescence signatures using a fluorescence imaging system (Speedzen, Beambio, France) described in details in (3), 19 meiotic products (24%) displayed the *pgrl1* signature (data not shown), and 17 meiotic products (23%) displayed the *hydg-2* signature (data not shown). We isolated five colonies (6% of the meiotic products) defective in PSI-CEF and hydrogenase activity (*C* and *D*). (E) Molecular

characterization of b1-21 meiotic product. We next determine if those meiotic products properly possess insertions of the resistance cassettes in *PGRL1* and *HYDG* genes. Total nucleic acids were prepared according to (4). PCR fragments were amplified from total DNA using *Taq* polymerase according to standard protocols. . PCR analysis for detecting the presence of interrupted *PGRL1* (*APHVIII* paromomycin resistance cassette at the level of first exon of the *PGRL1* gene as indicated in (1) and *HYDG* (*APHVII* hygromycin resistance cassette between nucleotide 48 and 153 of the *HYDG* gene as indicated in (2) genes in the wild type, the parental strains and the *pgrl1 hydg-2* double mutant (see material and method section for further details). (left) Amplification of an independent genomic fragment of similar size order (600 bp) is used as a positive control for DNA quality and reaction conditions. (middle) Amplification of a genomic fragment of *HYDG* gene yields an 800bp fragment in wild type. (right) Amplification of a genomic fragment of *PGRL1* gene yields an 900 bp fragment in wild type.

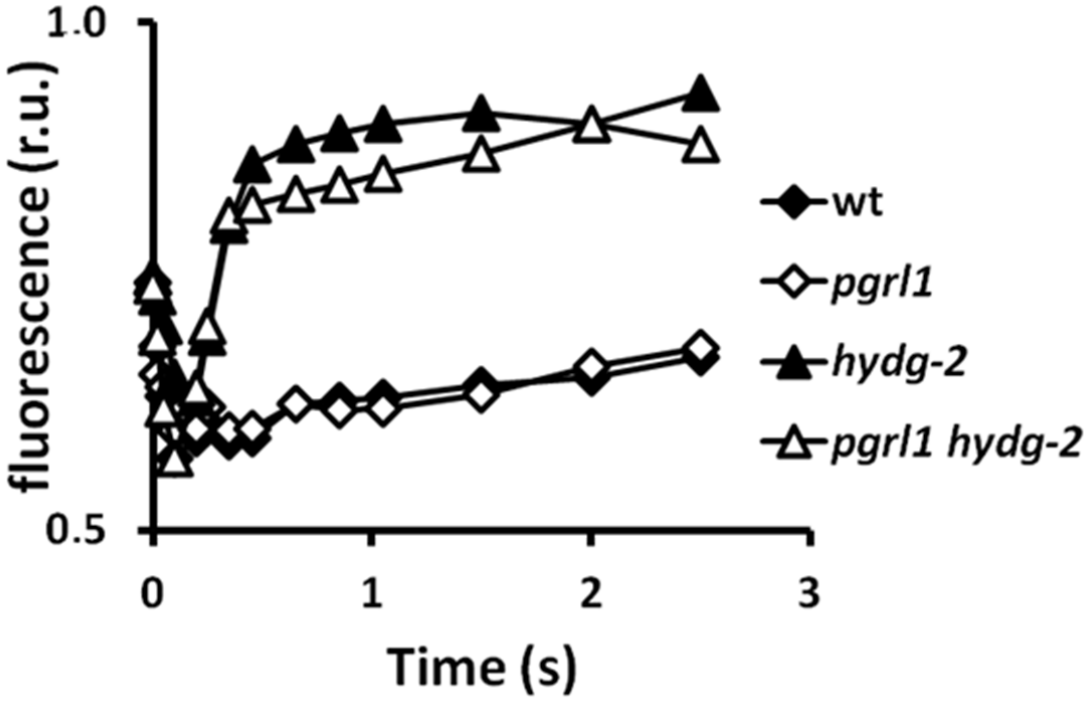

Supplemental Figure 2. **Chlorophyll fluorescence kinetics** of *Chlamydomonas reinhardtii pgrl1* (open diamonds)*, hydg-2* (dark triangles) and *pgrl1 hydg-2* (open triangles) mutants compared to wild type (dark diamonds) after one hours of dark anoxic conditions. According to (1), it indicates that hydrogenase is well expressed in wild type and *pgrl1*.

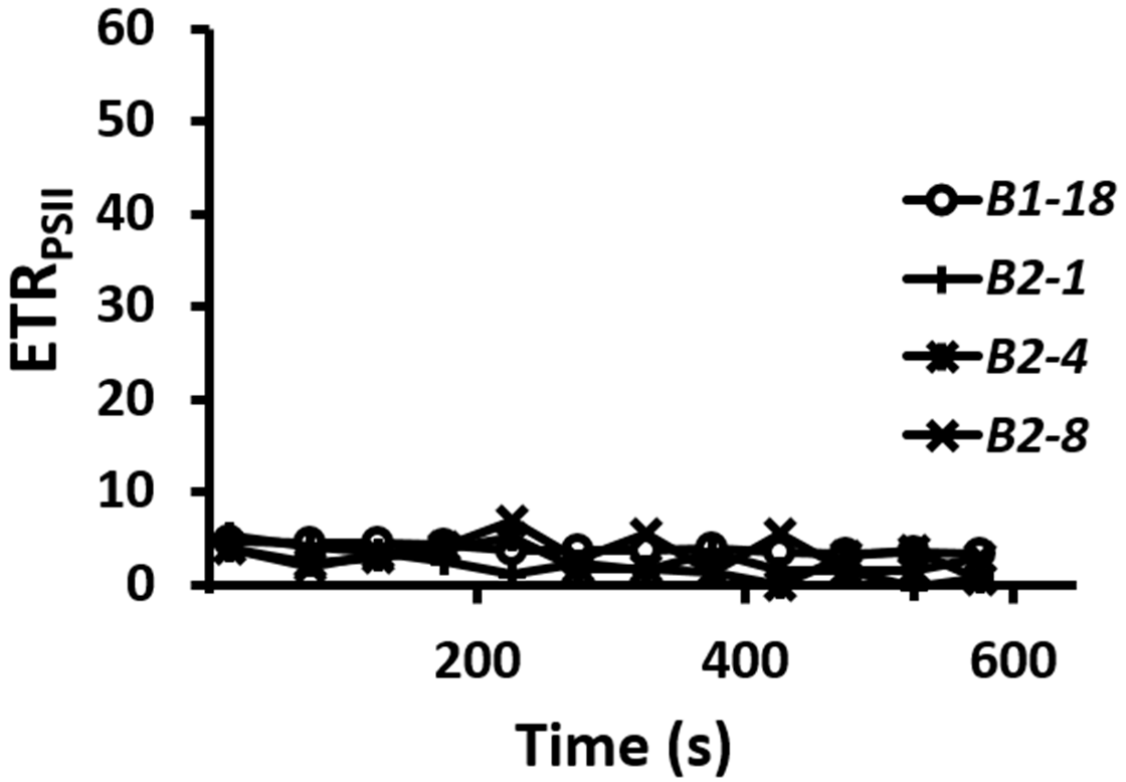

Supplemental Figure 3. **Photosystem II electron transfer rate upon a shift from dark-anoxia (1 hour) to light** in four double mutant meiotic products. ETR_{PSII} ($e^- \cdot s^{-1} \cdot PSII^{-1}$) remains null in every double mutants.

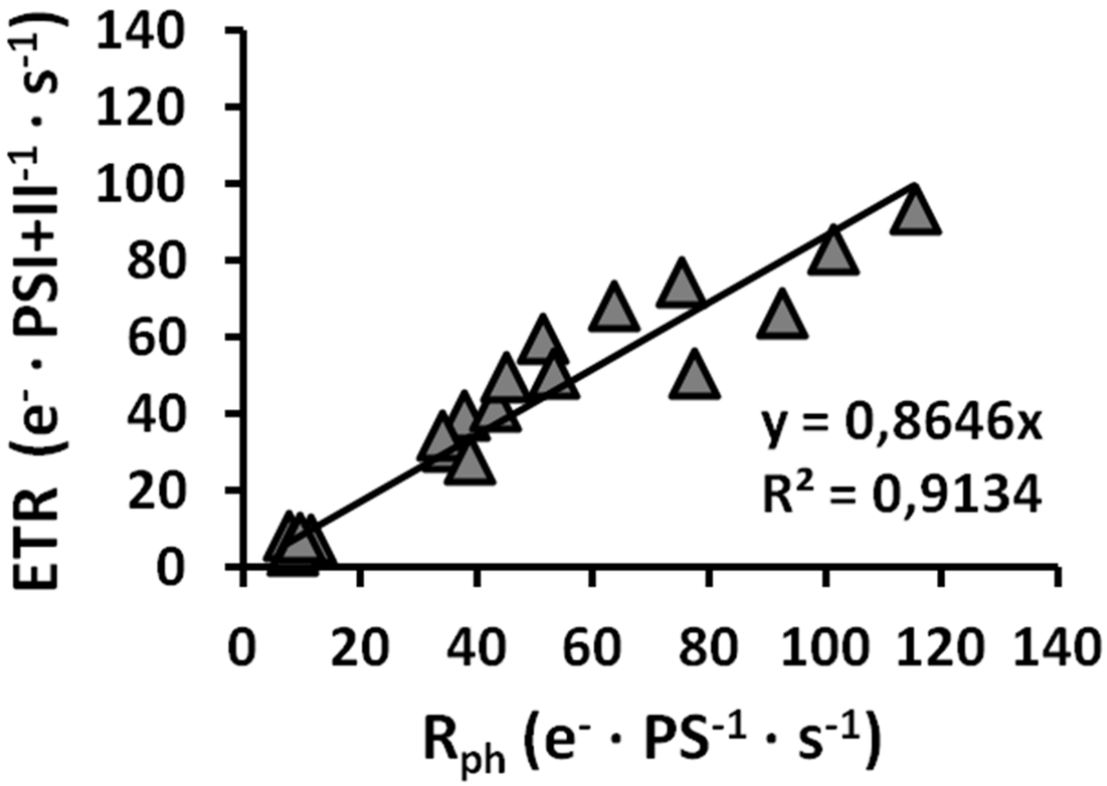

Supplemental Figure 4. **Relationship between photochemical rate** (R_{ph}) **and ETR** ($ETR_{PSII} + ETR_{PSI}$) of four strains (values taken from Figures 1 and 3). This relationship demonstrates that $ETR_{PSII} + ETR_{PSI} \sim 2\ R_{ph}$.

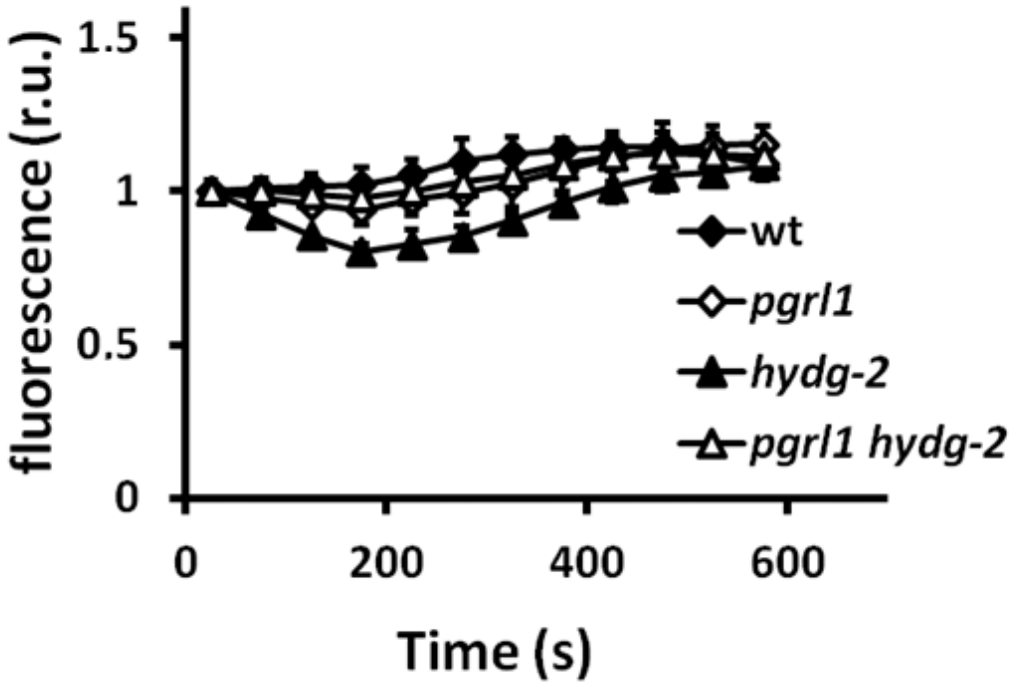

Supplemental Figure 5. **Maximal fluorescence yield (Fm') upon a shift from dark-anoxia to light** as a mean of assessing the occurrence of state transitions wild type (dark diamonds), *pgrl1* (open diamonds), *hydg-2* (dark triangles), and *pgrl1 hydg-2* (open triangles). All measurements were performed at least in triplicate (n ≥ 3) and data are presented as means ± SD. F_m' value at the onset of light was normalized to 1 (r.u. relative units).

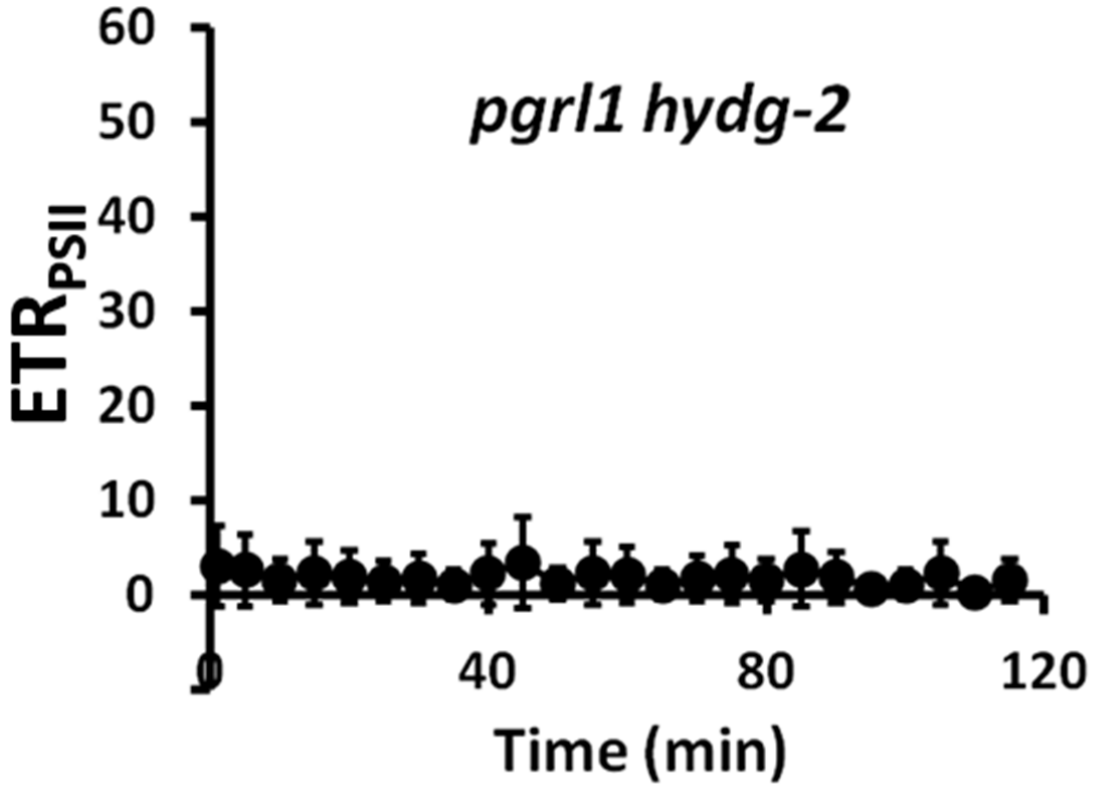

Supplemental Figure 6. **PSII electron transfer rate** (ETR_{PSII}, $e^- \cdot s^{-1} \cdot PSII^{-1}$) **upon a shift from dark-anoxia (1 hour) to light** in *pgrl1 hydg-2*. No significant PSII-driven electron flow could be detected even after 2 hours of illumination. All measurements were performed at least in triplicate ($n \geq 3$) and data are presented as means ± SD.

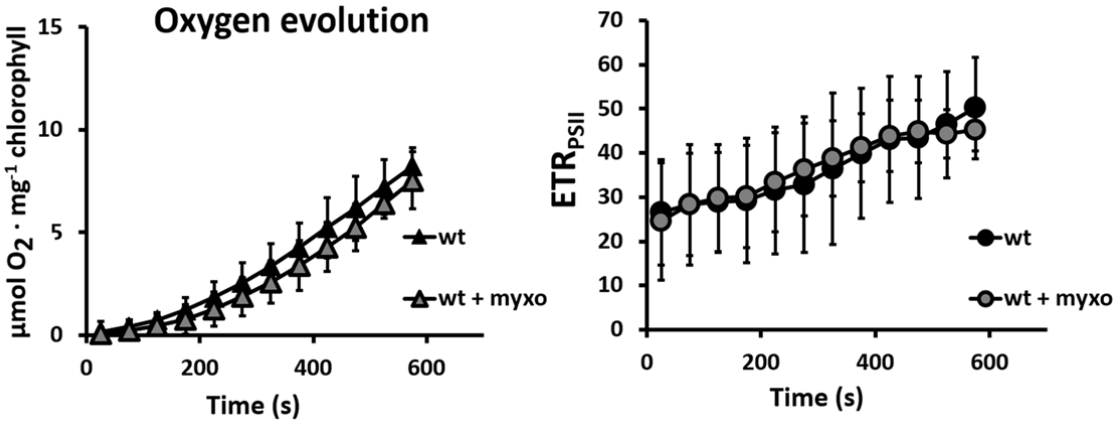

Supplemental Figure 7. **(A) Oxygen concentration** (µmol O_2 · mg^{-1} chlorophyll) **and (B) PSII electron transfer rate** (ETR_{PSII}, e^- · s^{-1} · $PSII^{-1}$) **upon a shift from dark anoxia (1 hour) to light** in wild type. Anoxia is reached by bubbling with nitrogen for 5 minutes prior incubation in the dark and, when needed, myxothiazol (myxo, 10µM) is added prior illumination. All measurements were performed at least in triplicate (n ≥ 3) and data are presented as means ± SD.

Supplemental information

Supplemental Figure 1. **Isolation of *pgrl1 hydg*-2 double mutants by a double chlorophyll fluorescence screen**. Double mutant *pgrl1 hydg-2* were obtained by crossing the *pgrl1 mt*$^{-}$ mutant with the *hydg-2 mt+* mutant and meiotic progeny was selected on TAP medium containing 25 mg/l hygromycin-B and 10 mg/l paromomycin. Both parental strains have been isolated on the basis of peculiar chlorophyll fluorescence kinetics, respectively in oxic conditions for *pgrl1* (*A*) (1) and in anoxic conditions for *hydg-2* (B) (2). Out of 78 meiotic products screened for both specific fluorescence signatures using a fluorescence imaging system (Speedzen, Beambio, France) described in details in (3), 19 meiotic products (24%) displayed the *pgrl1* signature (data not shown), and 17 meiotic products (23%) displayed the *hydg-2* signature (data not shown). We isolated five colonies (6% of the meiotic products) defective in PSI-CEF and hydrogenase activity (*C* and *D*). (E) Molecular characterization of b1-21 meiotic product. We next determine if those meiotic products properly possess insertions of the resistance cassettes in *PGRL1* and *HYDG* genes. Total nucleic acids were prepared according to (4). PCR fragments were amplified from total DNA using *Taq* polymerase according to standard protocols. . PCR analysis for detecting the presence of interrupted *PGRL1* (*APHVIII* paromomycin resistance cassette at the level of first exon of the *PGRL1* gene as indicated in (1) and *HYDG* (*APHVII* hygromycin resistance cassette between nucleotide 48 and 153 of the *HYDG* gene as indicated in (2) genes in the wild type, the parental strains and the *pgrl1 hydg-2* double mutant (see material and method section for further details). (left) Amplification of an independent genomic fragment of similar size order (600 bp) is used as a positive control for DNA quality and reaction conditions. (middle) Amplification of a genomic fragment of *HYDG* gene yields an 800bp fragment in wild type. (right) Amplification of a genomic fragment of *PGRL1* gene yields an 900 bp fragment in wild type.

Supplemental Figure 2. **Chlorophyll fluorescence kinetics** of *Chlamydomonas reinhardtii pgrl1* (open diamonds)*, hydg-2* (dark triangles) and *pgrl1 hydg-2* (open triangles) mutants compared to wild type (dark diamonds) after one hours of dark anoxic conditions. According to (1), it indicates that hydrogenase is well expressed in wild type and *pgrl1*.

Supplemental Figure 3. **Photosystem II electron transfer rate upon a shift from dark-anoxia (1 hour) to light** in four double mutant meiotic products. ETR_{PSII} ($e^{-} \cdot s^{-1} \cdot PSII^{-1}$) remains null in every double mutants.

Supplemental Figure 4. **Relationship between photochemical rate** (R_{ph}) **and ETR** ($ETR_{PSII} + ETR_{PSI}$) of four strains (values taken from Figures 1 and 3). This relationship demonstrates that $ETR_{PSII} + ETR_{PSI} \sim 2\ R_{ph}$.

Supplemental Figure 5. **Maximal fluorescence yield (Fm') upon a shift from dark-anoxia to light** as a mean of assessing the occurrence of state transitions wild type (dark diamonds), *pgrl1* (open diamonds), *hydg-2* (dark triangles), and *pgrl1 hydg-2* (open triangles). All measurements were performed at least in triplicate ($n \geq 3$) and data are presented as means ± SD. F_m' value at the onset of light was normalized to 1 (r.u. relative units).

Supplemental Figure 6. **PSII electron transfer rate** (ETR_{PSII}, $e^- \cdot s^{-1} \cdot PSII^{-1}$) **upon a shift from dark-anoxia (1 hour) to light** in *pgrl1 hydg-2*. No significant PSII-driven electron flow could be detected even after 2 hours of illumination. All measurements were performed at least in triplicate ($n \geq 3$) and data are presented as means ± SD.

Supplemental Figure 7. **(A) Oxygen concentration** (µmol $O_2 \cdot mg^{-1}$ chlorophyll) **and (B) PSII electron transfer rate** (ETR_{PSII}, $e^- \cdot s^{-1} \cdot PSII^{-1}$) **upon a shift from dark anoxia (1 hour) to light** in wild type. Anoxia is reached by bubbling with nitrogen for 5 minutes prior incubation in the dark and, when needed, myxothiazol (myxo, 10µM) is added prior illumination. All measurements were performed at least in triplicate ($n \geq 3$) and data are presented as means ± SD.

1. Tolleter D*, et al.* (2011) Control of hydrogen photoproduction by the proton gradient generated by cyclic electron flow in Chlamydomonas reinhardtii. *The Plant cell* 23(7):2619-2630.
2. Godaux D*, et al.* (2013) A novel screening method for hydrogenase-deficient mutants in Chlamydomonas reinhardtii based on in vivo chlorophyll fluorescence and photosystem II quantum yield. *International journal of hydrogen energy* 38(4):1826-1836.
3. Johnson X*, et al.* (2009) A new setup for in vivo fluorescence imaging of photosynthetic activity. *Photosynthesis research* 102(1):85-93.
4. Neuwman SM*, et al.* (1990) Transformation of chloroplast ribosomal RNA genes in Chlamydomonas: molecular and genetic characterization of integration events. *Genetics* 126:875-888.

Parsed Citations

Allen, J.F. (2003). Cyclic, pseudocyclic and noncyclic photophosphorylation: new links in the chain. Trends Plant Sci 8: 15-19.
Pubmed: Author and Title
CrossRef: Author and Title
Google Scholar: Author Only Title Only Author and Title

Alric, J. (2010). Cyclic electron flow around photosystem I in unicellular green algae. Photosynth Res 106: 47-56.
Pubmed: Author and Title
CrossRef: Author and Title
Google Scholar: Author Only Title Only Author and Title

Alric, J. (2014). Redox and ATP control of photosynthetic cyclic electron flow in Chlamydomonas reinhardtii: (II) involvement of the PGR5-PGRL1 pathway under anaerobic conditions. Biochim Biophys Acta 1837: 825-834.
Pubmed: Author and Title
CrossRef: Author and Title
Google Scholar: Author Only Title Only Author and Title

Appel, J., Phunpruch, S., Steinmuller, K. and Schulz, R. (2000). The bidirectional hydrogenase of Synechocystis sp. PCC 6803 works as an electron valve during photosynthesis. Arch Microbiol 173: 333-338.
Pubmed: Author and Title
CrossRef: Author and Title
Google Scholar: Author Only Title Only Author and Title

Arnon, D.I. (1955). The chloroplast as a complete photosynthetic unit. Science 122: 9-16.
Pubmed: Author and Title
CrossRef: Author and Title
Google Scholar: Author Only Title Only Author and Title

Bailleul, B., Cardol, P., Breyton, C. and Finazzi, G. (2010). Electrochromism: a useful probe to study algal photosynthesis. Photosynth Res 106: 179-189.
Pubmed: Author and Title
CrossRef: Author and Title
Google Scholar: Author Only Title Only Author and Title

Baltz, A., Dang, K.V., Beyly, A., Auroy, P., Richaud, P., Cournac, L. and Peltier, G. (2014). Plastidial Expression of Type II NAD(P)H Dehydrogenase Increases the Reducing State of Plastoquinones and Hydrogen Photoproduction Rate by the Indirect Pathway in Chlamydomonas reinhardtii1. Plant Physiol 165: 1344-1352.
Pubmed: Author and Title
CrossRef: Author and Title
Google Scholar: Author Only Title Only Author and Title

Barz, M. et al. (2010). Distribution analysis of hydrogenases in surface waters of marine and freshwater environments. PLoS One 5: e13846.
Pubmed: Author and Title
CrossRef: Author and Title
Google Scholar: Author Only Title Only Author and Title

Bennoun, P. (1982). Evidence for a respiratory chain in the chloroplast. Proc Natl Acad Sci U S A 79: 4352-4356.
Pubmed: Author and Title
CrossRef: Author and Title
Google Scholar: Author Only Title Only Author and Title

Cardol, P., Alric, J., Girard-Bascou, J., Franck, F., Wollman, F.A. and Finazzi, G. (2009). Impaired respiration discloses the physiological significance of state transitions in Chlamydomonas. Proc Natl Acad Sci U S A 106: 15979-15984.
Pubmed: Author and Title
CrossRef: Author and Title
Google Scholar: Author Only Title Only Author and Title

Cardol, P., Forti, G. and Finazzi, G. (2011). Regulation of electron transport in microalgae. Biochim Biophys Acta 1807: 912-918.
Pubmed: Author and Title
CrossRef: Author and Title
Google Scholar: Author Only Title Only Author and Title

Carrieri, D., Wawrousek, K., Eckert, C., Yu, J. and Maness, P.C. (2011). The role of the bidirectional hydrogenase in cyanobacteria. Bioresour Technol 102: 8368-8377.
Pubmed: Author and Title
CrossRef: Author and Title
Google Scholar: Author Only Title Only Author and Title

Clowez, S., Godaux, D., Cardol, P., Wollman, F.A. and Rappaport, F. (2015). The Involvement of Hydrogen-producing and ATP-dependent NADPH-consuming Pathways in Setting the Redox Poise in the Chloroplast of Chlamydomonas reinhardtii in Anoxia. J Biol Chem 290: 8666-8676.
Pubmed: Author and Title
CrossRef: Author and Title
Google Scholar: Author Only Title Only Author and Title

Cohen, J., Kim, K., Posewitz, M., Ghirardi, M.L., Schulten, K., Seibert, M. and King, P. (2005). Molecular dynamics and experimental investigation of H(2) and O(2) diffusion in [Fe]-hydrogenase. Biochem Soc Trans 33: 80-82.
Pubmed: Author and Title

CrossRef: Author and Title
Google Scholar: Author Only Title Only Author and Title

Cournac, L., Guedeney, G., Peltier, G. and Vignais, P.M. (2004). Sustained photoevolution of molecular hydrogen in a mutant of Synechocystis sp. strain PCC 6803 deficient in the type I NADPH-dehydrogenase complex. J Bacteriol 186: 1737-1746.
Pubmed: Author and Title
CrossRef: Author and Title
Google Scholar: Author Only Title Only Author and Title

Cournac, L., Mus, F., Bernard, L., Guedeney, G., Vignais, P.M. and Peltier, G. (2002). Limiting steps of hydrogen production in Chlamydomonas reinhardtii and Synechocystis PCC 6803 as analysed by light-induced gas exchange transients. International Journal of Hydrogen Energy 27: 1229-1237.
Pubmed: Author and Title
CrossRef: Author and Title
Google Scholar: Author Only Title Only Author and Title

DalCorso, G., Pesaresi, P., Masiero, S., Aseeva, E., Schunemann, D., Finazzi, G., Joliot, P., Barbato, R. and Leister, D. (2008). A complex containing PGRL1 and PGR5 is involved in the switch between linear and cyclic electron flow in Arabidopsis. Cell 132: 273-285.
Pubmed: Author and Title
CrossRef: Author and Title
Google Scholar: Author Only Title Only Author and Title

Dang, K.V., Plet, J., Tolleter, D., Jokel, M., Cuine, S., Carrier, P., Auroy, P., Richaud, P., Johnson, X., Alric, J., Allahverdiyeva, Y. and Peltier, G. (2014). Combined Increases in Mitochondrial Cooperation and Oxygen Photoreduction Compensate for Deficiency in Cyclic Electron Flow in Chlamydomonas reinhardtii. Plant Cell 26: 3036-3050.
Pubmed: Author and Title
CrossRef: Author and Title
Google Scholar: Author Only Title Only Author and Title

Florin, L., Tsokoglou, A. and Happe, T. (2001). A novel type of iron hydrogenase in the green alga Scenedesmus obliquus is linked to the photosynthetic electron transport chain. J Biol Chem 276: 6125-6132.
Pubmed: Author and Title
CrossRef: Author and Title
Google Scholar: Author Only Title Only Author and Title

Forestier, M., King, P., Zhang, L., Posewitz, M., Schwarzer, S., Happe, T., Ghirardi, M.L. and Seibert, M. (2003). Expression of two [Fe]-hydrogenases in Chlamydomonas reinhardtii under anaerobic conditions. Eur J Biochem 270: 2750-2758.
Pubmed: Author and Title
CrossRef: Author and Title
Google Scholar: Author Only Title Only Author and Title

Ghirardi, M.L., Dubini, A., Yu, J. and Maness, P.C. (2009). Photobiological hydrogen-producing systems. Chem Soc Rev 38: 52-61.
Pubmed: Author and Title
CrossRef: Author and Title
Google Scholar: Author Only Title Only Author and Title

Ghirardi, M.L., Togasaki, R.K. and Seibert, M. (1997). Oxygen sensitivity of algal H2- production. Appl Biochem Biotechnol 63-65: 141-151.
Pubmed: Author and Title
CrossRef: Author and Title
Google Scholar: Author Only Title Only Author and Title

Ghysels, B., Godaux, D., Matagne, R.F., Cardol, P. and Franck, F. (2013). Function of the chloroplast hydrogenase in the microalga Chlamydomonas: the role of hydrogenase and state transitions during photosynthetic activation in anaerobiosis. PLoS One 8: e64161.
Pubmed: Author and Title
CrossRef: Author and Title
Google Scholar: Author Only Title Only Author and Title

Godaux, D., Emonds-Alt, B., Berne, N., Ghysels, B., Alric, J., Remacle, C. and Cardol, P. (2013). A novel screening method for hydrogenase-deficient mutants in Chlamydomonas reinhardtii based on in vivo chlorophyll fluorescence and photosystem II quantum yield. International Journal of Hydrogen Energy 38: 1826-1836.
Pubmed: Author and Title
CrossRef: Author and Title
Google Scholar: Author Only Title Only Author and Title

Grossman, A.R., Catalanotti, C., Yang, W., Dubini, A., Magneschi, L., Subramanian, V., Posewitz, M.C. and Seibert, M. (2011). Multiple facets of anoxic metabolism and hydrogen production in the unicellular green alga Chlamydomonas reinhardtii. New Phytol 190: 279-288.
Pubmed: Author and Title
CrossRef: Author and Title
Google Scholar: Author Only Title Only Author and Title

Happe, T. and Naber, J.D. (1993). Isolation, characterization and N-terminal amino acid sequence of hydrogenase from the green alga Chlamydomonas reinhardtii. Eur J Biochem 214: 475-481.
Pubmed: Author and Title
CrossRef: Author and Title
Google Scholar: Author Only Title Only Author and Title

Harbinson, J., Genty, B. and Foyer, C. (1990). Relationship between Photosynthetic Electron Transport

and Stromal Enzyme Activity in Pea Leaves: Toward an Understanding of the Nature of Photosynthetic Control. Plant Physiol 94: 545-553.

Hertle, A.P., Blunder, T., Wunder, T., Pesaresi, P., Pribil, M., Armbruster, U. and Leister, D. (2013). PGRL1 is the elusive ferredoxin-plastoquinone reductase in photosynthetic cyclic electron flow. Mol Cell 49: 511-523.
Pubmed: Author and Title
CrossRef: Author and Title
Google Scholar: Author Only Title Only Author and Title

Houille-Vernes, L., Rappaport, F., Wollman, F.A., Alric, J. and Johnson, X. (2011). Plastid terminal oxidase 2 (PTOX2) is the major oxidase involved in chlororespiration in Chlamydomonas. Proc Natl Acad Sci U S A 108: 20820-20825.
Pubmed: Author and Title
CrossRef: Author and Title
Google Scholar: Author Only Title Only Author and Title

Iwai, M., Takizawa, K., Tokutsu, R., Okamuro, A., Takahashi, Y. and Minagawa, J. (2010). Isolation of the elusive supercomplex that drives cyclic electron flow in photosynthesis. Nature 464: 1210-1213.
Pubmed: Author and Title
CrossRef: Author and Title
Google Scholar: Author Only Title Only Author and Title

Jacquot, J.P., Stein, M., Suzuki, A., Liottet, S., Sandoz, G. and Miginiac-Maslow, M. (1997). Residue Glu-91 of Chlamydomonas reinhardtii ferredoxin is essential for electron transfer to ferredoxin-thioredoxin reductase. FEBS Lett 400: 293-296.
Pubmed: Author and Title
CrossRef: Author and Title
Google Scholar: Author Only Title Only Author and Title

Jans, F., Mignolet, E., Houyoux, P.A., Cardol, P., Ghysels, B., Cuine, S., Cournac, L., Peltier, G., Remacle, C. and Franck, F. (2008). A type II NAD(P)H dehydrogenase mediates light-independent plastoquinone reduction in the chloroplast of Chlamydomonas. Proc Natl Acad Sci U S A 105: 20546-20551.
Pubmed: Author and Title
CrossRef: Author and Title
Google Scholar: Author Only Title Only Author and Title

Johnson, G.N. (2011). Reprint of: physiology of PSI cyclic electron transport in higher plants. Biochim Biophys Acta 1807: 906-911.
Pubmed: Author and Title
CrossRef: Author and Title
Google Scholar: Author Only Title Only Author and Title

Johnson, X. and Alric, J. (2012). Interaction between starch breakdown, acetate assimilation, and photosynthetic cyclic electron flow in Chlamydomonas reinhardtii. J Biol Chem 287: 26445-26452.
Pubmed: Author and Title
CrossRef: Author and Title
Google Scholar: Author Only Title Only Author and Title

Johnson, X. and Alric, J. (2013). Central carbon metabolism and electron transport in Chlamydomonas reinhardtii: metabolic constraints for carbon partitioning between oil and starch. Eukaryot Cell 12: 776-793.
Pubmed: Author and Title
CrossRef: Author and Title
Google Scholar: Author Only Title Only Author and Title

Johnson, X. et al. (2014). Proton gradient regulation 5-mediated cyclic electron flow under ATP- or redox-limited conditions: a study of DeltaATpase pgr5 and DeltarbcL pgr5 mutants in the green alga Chlamydomonas reinhardtii. Plant Physiol 165: 438-452.
Pubmed: Author and Title
CrossRef: Author and Title
Google Scholar: Author Only Title Only Author and Title

Joliot, P. and Johnson, G.N. (2011). Regulation of cyclic and linear electron flow in higher plants. Proc Natl Acad Sci U S A 108: 13317-13322.
Pubmed: Author and Title
CrossRef: Author and Title
Google Scholar: Author Only Title Only Author and Title

Joliot, P. and Joliot, A. (2002). Cyclic electron transfer in plant leaf. Proc Natl Acad Sci U S A 99: 10209-10214.
Pubmed: Author and Title
CrossRef: Author and Title
Google Scholar: Author Only Title Only Author and Title

Kessler, E. (1973). Effect of anaerobiosis on photosynthetic reactions and nitrogen metabolism of algae with and without hydrogenase. Arch Mikrobiol 93: 91-100.
Pubmed: Author and Title
CrossRef: Author and Title
Google Scholar: Author Only Title Only Author and Title

Klughammer, B. and Schreiber, U. (2008). Saturation pulse method for assessment of energy conversion in

PSI. PAM application Notes 1: 11-14.

Kolber, Z. and Falkowski, P.G. (1993). Use of active fluorescence to estimate phytoplankton photosynthesis in situ. Limnol

Oceanogr 38: 1646-1665.
Pubmed: Author and Title
CrossRef: Author and Title
Google Scholar: Author Only Title Only Author and Title

Kruse, O., Rupprecht, J., Bader, K.P., Thomas-Hall, S., Schenk, P.M., Finazzi, G. and Hankamer, B. (2005). Improved photobiological H2 production in engineered green algal cells. J Biol Chem 280: 34170-34177.
Pubmed: Author and Title
CrossRef: Author and Title
Google Scholar: Author Only Title Only Author and Title

Kukuczka, B., Magneschi, L., Petroutsos, D., Steinbeck, J., Bald, T., Powikrowska, M., Fufezan, C., Finazzi, G. and Hippler, M. (2014). Proton Gradient Regulation5-Like1-Mediated Cyclic Electron Flow Is Crucial for Acclimation to Anoxia and Complementary to Nonphotochemical Quenching in Stress Adaptation. Plant Physiol 165: 1604-1617.
Pubmed: Author and Title
CrossRef: Author and Title
Google Scholar: Author Only Title Only Author and Title

Lavergne, J. (1989). Mitochondrial responses to intracellular pulses of photosynthetic oxygen. Proc Natl Acad Sci U S A 86: 8768-8772.
Pubmed: Author and Title
CrossRef: Author and Title
Google Scholar: Author Only Title Only Author and Title

Leister, D. and Shikanai, T. (2013). Complexities and protein complexes in the antimycin A-sensitive pathway of cyclic electron flow in plants. Front Plant Sci 4: 161.
Pubmed: Author and Title
CrossRef: Author and Title
Google Scholar: Author Only Title Only Author and Title

Lemeille, S. and Rochaix, J.D. (2010). State transitions at the crossroad of thylakoid signalling pathways. Photosynth Res 106: 33-46.
Pubmed: Author and Title
CrossRef: Author and Title
Google Scholar: Author Only Title Only Author and Title

Lucker, B. and Kramer, D.M. (2013). Regulation of cyclic electron flow in Chlamydomonas reinhardtii under fluctuating carbon availability. Photosynth Res 117: 449-459.
Pubmed: Author and Title
CrossRef: Author and Title
Google Scholar: Author Only Title Only Author and Title

Melis, A., Zhang, L., Forestier, M., Ghirardi, M.L. and Seibert, M. (2000). Sustained photobiological hydrogen gas production upon reversible inactivation of oxygen evolution in the green alga Chlamydomonas reinhardtii. Plant Physiol 122: 127-136.
Pubmed: Author and Title
CrossRef: Author and Title
Google Scholar: Author Only Title Only Author and Title

Miyake, C. (2010). Alternative electron flows (water-water cycle and cyclic electron flow around PSI) in photosynthesis: molecular mechanisms and physiological functions. Plant Cell Physiol 51: 1951-1963.
Pubmed: Author and Title
CrossRef: Author and Title
Google Scholar: Author Only Title Only Author and Title

Mus, F., Dubini, A., Seibert, M., Posewitz, M.C. and Grossman, A.R. (2007). Anaerobic acclimation in Chlamydomonas reinhardtii: anoxic gene expression, hydrogenase induction, and metabolic pathways. J Biol Chem 282: 25475-25486.
Pubmed: Author and Title
CrossRef: Author and Title
Google Scholar: Author Only Title Only Author and Title

Nagy, G., Unnep, R., Zsiros, O., Tokutsu, R., Takizawa, K., Porcar, L., Moyet, L., Petroutsos, D., Garab, G., Finazzi, G. and Minagawa, J. (2014). Chloroplast remodeling during state transitions in Chlamydomonas reinhardtii as revealed by noninvasive techniques in vivo. Proc Natl Acad Sci U S A 111: 5042-5047.
Pubmed: Author and Title
CrossRef: Author and Title
Google Scholar: Author Only Title Only Author and Title

Pape, M., Lambertz, C., Happe, T. and Hemschemeier, A. (2012). Differential expression of the Chlamydomonas [FeFe]-hydrogenase-encoding HYDA1 gene is regulated by the copper response regulator1. Plant Physiol 159: 1700-1712.
Pubmed: Author and Title
CrossRef: Author and Title
Google Scholar: Author Only Title Only Author and Title

Peltier, G., Tolleter, D., Billon, E. and Cournac, L. (2010). Auxiliary electron transport pathways in chloroplasts of microalgae. Photosynth Res 106: 19-31.
Pubmed: Author and Title
CrossRef: Author and Title
Google Scholar: Author Only Title Only Author and Title

Posewitz, M.C., King, P.W., Smolinski, S.L., Zhang, L., Seibert, M. and Ghirardi, M.L. (2004). Discovery of two novel radical S-

adenosylmethionine proteins required for the assembly of an active [Fe] hydrogenase. J Biol Chem 279: 25711-25720.
Pubmed: Author and Title
CrossRef: Author and Title
Google Scholar: Author Only Title Only Author and Title

Ral, J.P., Colleoni, C., Wattebled, F., Dauvillee, D., Nempont, C., Deschamps, P., Li, Z., Morell, M.K., Chibbar, R., Purton, S., d'Hulst, C. and Ball, S.G. (2006). Circadian clock regulation of starch metabolism establishes GBSSI as a major contributor to amylopectin synthesis in Chlamydomonas reinhardtii. Plant Physiol 142: 305-317.
Pubmed: Author and Title
CrossRef: Author and Title
Google Scholar: Author Only Title Only Author and Title

Ruhle, T., Hemschemeier, A., Melis, A. and Happe, T. (2008). A novel screening protocol for the isolation of hydrogen producing Chlamydomonas reinhardtii strains. BMC Plant Biol 8: 107.
Pubmed: Author and Title
CrossRef: Author and Title
Google Scholar: Author Only Title Only Author and Title

Schreiber, U. and Vidaver, W. (1974). Chlorophyll fluorescence induction in anaerobic Scenedesmus obliquus. Biochim Biophys Acta 368: 97-112.
Pubmed: Author and Title
CrossRef: Author and Title
Google Scholar: Author Only Title Only Author and Title

Sicher, R.C. (1984). Characteristics of light-dependent inorganic carbon uptake by isolated spinach chloroplasts. Plant Physiol 74: 962-966.
Pubmed: Author and Title
CrossRef: Author and Title
Google Scholar: Author Only Title Only Author and Title

Takahashi, H., Clowez, S., Wollman, F.A., Vallon, O. and Rappaport, F. (2013). Cyclic electron flow is redox-controlled but independent of state transition. Nat Commun 4: 1954.
Pubmed: Author and Title
CrossRef: Author and Title
Google Scholar: Author Only Title Only Author and Title

Terashima, M., Specht, M., Naumann, B. and Hippler, M. (2010). Characterizing the anaerobic response of Chlamydomonas reinhardtii by quantitative proteomics. Mol Cell Proteomics 9: 1514-1532.
Pubmed: Author and Title
CrossRef: Author and Title
Google Scholar: Author Only Title Only Author and Title

Tikkanen, M., Grieco, M., Nurmi, M., Rantala, M., Suorsa, M. and Aro, E.M. (2012). Regulation of the photosynthetic apparatus under fluctuating growth light. Philos Trans R Soc Lond B Biol Sci 367: 3486-3493.
Pubmed: Author and Title
CrossRef: Author and Title
Google Scholar: Author Only Title Only Author and Title

Tolleter, D. et al. (2011). Control of hydrogen photoproduction by the proton gradient generated by cyclic electron flow in Chlamydomonas reinhardtii. Plant Cell 23: 2619-2630.
Pubmed: Author and Title
CrossRef: Author and Title
Google Scholar: Author Only Title Only Author and Title

Unlu, C., Drop, B., Croce, R. and van Amerongen, H. (2014). State transitions in Chlamydomonas reinhardtii strongly modulate the functional size of photosystem II but not of photosystem I. Proc Natl Acad Sci U S A 111: 3460-3465.
Pubmed: Author and Title
CrossRef: Author and Title
Google Scholar: Author Only Title Only Author and Title

Witt, H., Bordignon, E., Carbonera, D., Dekker, J.P., Karapetyan, N., Teutloff, C., Webber, A., Lubitz, W. and Schlodder, E. (2003). Species-specific differences of the spectroscopic properties of P700: analysis of the influence of non-conserved amino acid residues by site-directed mutagenesis of photosystem I from Chlamydomonas reinhardtii. J Biol Chem 278: 46760-46771.
Pubmed: Author and Title
CrossRef: Author and Title
Google Scholar: Author Only Title Only Author and Title

Wollman, F.A. and Delepelaire, P. (1984). Correlation between changes in light energy distribution and changes in thylakoid membrane polypeptide phosphorylation in Chlamydomonas reinhardtii. J Cell Biol 98: 1-7.
Pubmed: Author and Title
CrossRef: Author and Title
Google Scholar: Author Only Title Only Author and Title

Yacoby, I., Pochekailov, S., Toporik, H., Ghirardi, M.L., King, P.W. and Zhang, S. (2011). Photosynthetic electron partitioning between [FeFe]-hydrogenase and ferredoxin:NADP+-oxidoreductase (FNR) enzymes in vitro. Proc Natl Acad Sci U S A 108: 9396-9401.
Pubmed: Author and Title
CrossRef: Author and Title
Google Scholar: Author Only Title Only Author and Title

Yang, W., Catalanotti, C., Posewitz, M., Alric, J. and Grossman, A. (2014). Insights into Algal Fermentation. In: van Dongen JT, Licausi F (eds) Low-Oxygen Stress in Plants. Plant Cell Monographs, vol 21. Springer Vienna, pp 135-163.
Pubmed: Author and Title
CrossRef: Author and Title
Google Scholar: Author Only Title Only Author and Title

Yoshida, K., Watanabe, C.K., Terashima, I. and Noguchi, K. (2011). Physiological impact of mitochondrial alternative oxidase on photosynthesis and growth in Arabidopsis thaliana. Plant Cell Environ 34: 1890-1899.
Pubmed: Author and Title
CrossRef: Author and Title
Google Scholar: Author Only Title Only Author and Title